

A study of semileptonic B decays

Doctoral Thesis of Piotr Urban

June 2000

Institute of Physics, University of Silesia, Katowice,
Poland

I would like to thank my advisor,
Professor Marek Jeżabek,
for essential help with this work.

A study of semileptonic B decays.

Piotr Urban

Institute of Physics, University of Silesia,
ul. Uniwersytecka 4, PL-40007 Katowice, Poland.

Abstract

Perturbative and nonperturbative QCD corrections to semileptonic B decay rates are calculated and given in analytical and numerical forms. We present the analytic expression for the double distribution in hadronic mass and electron energy in $B \rightarrow X_u e \bar{\nu}_e$ decays through one loop order of QCD. We then study the leading twist corrections to that quantity within the formalism of HQET and employ it in a proposed method of measuring V_{ub} with an accuracy of 10%. Our other point of interest is the polarisation of the τ lepton in $B \rightarrow X_c \tau \bar{\nu}_\tau$ processes. Analytic formulae are given for the one-loop QCD correction to the longitudinal polarisation. The resulting moments of distributions are discussed, incorporating the HQET corrections found by Falk et al. The polarisation receives only a very small perturbative correction. It can be used in extracting the quark masses. Experimental considerations led us to the calculation of corrections to the polarisation of τ with respect to the momentum of the virtual W boson. Analytical results for the $\mathcal{O}(1/m_b^2)$ terms have been combined with numerically evaluated perturbative contributions to give the corrected polarisation.

Contents

1	Introduction	3
2	Kinematics	7
2.1	Variables	7
2.2	Kinematic boundaries	9
2.2.1	Partonic limits	9
2.2.2	Partonic limits - massless case	10
2.2.3	Meson kinematic boundaries	10
3	Evaluation of corrections	11
3.1	Perturbative corrections	11
3.2	Nonperturbative corrections	12
3.2.1	Corrections of order $1/m_b^2$	13
3.2.2	Leading twist approximation	14
3.2.3	Discussion of Fermi motion	14
4	Spectrum of hadronic mass and electron energy	17
4.1	Introduction	17
4.2	Evaluation	17
4.3	Analytical results	19
4.4	Moments	21
4.5	Summary	22
5	Extraction of V_{ub} from B decays	24
5.1	Introduction	24
5.2	Method of measuring V_{ub}	25
5.3	Combining perturbative and nonperturbative corrections	27
5.4	Shape function parameters	29
5.5	Results	31
5.5.1	General result on $ V_{ub} $ accuracy.	31
5.5.2	Partonic results.	33
5.5.3	Convolved partonic results.	35
5.5.4	Convolved one-loop corrections.	36
5.5.5	Perturbative and nonperturbative corrections.	37
5.5.6	Discussion of uncertainty.	37
5.6	Summary	38
6	Longitudinal polarisation of τ lepton	40
6.1	Introduction	40
6.2	Evaluation	44
6.3	Analytical results	46
6.4	Moments of τ energy distribution	53
6.5	Summary	56

7	Polarisation of τ lepton with respect to W	57
7.1	Introduction	57
7.2	Kinematics	57
7.3	Polarisation evaluation	58
7.4	Double differential distribution	60
7.5	Lepton energy distribution	62
7.6	Summary	66
8	Summary	68
9	Acknowledgements	68

1 Introduction

Semileptonic B decays form one of the most vigorously expanding branch of the studies of the Standard Model (SM), the current theory of elementary interactions [1, 2, 3] that has stood the test of some 20 years of experimental verification. This model is based on the concept of quantum field theory, developed at the time of creation of quantum electrodynamics [4, 5, 6]. It has thus built on and extended the perturbative [7, 8, 9, 10, 11] as well as nonperturbative [12, 13, 14, 15, 16, 17, 18, 19, 20, 21, 22] methods of field theory. For all its success, however, SM is far from completely describing the fundamental laws of nature. Even if we refrain from listing the nondiscovery of the Higgs boson as a liability, we are nonetheless left with a plethora of questions of theoretical nature. One of them is the origin of the values of the masses entering the model as well as the no less enigmatic entries of the Cabibbo-Kobayashi-Maskawa mixing matrix. The latter are connected with the topical problem of CP violation. Whereas there exist theories that attempt to provide a deeper insight on these, like supersymmetry and superstrings, the main obstacle often does not seem to lie so much with any lack of ideas as with exact measurement and precise theoretical prediction. The latter issue is due to the high level of complication characterising SM (not to mention any extension thereof) as well as the relatively large value of the strong coupling constant. The strong interactions cause trouble even in the description of the so-called weak processes due to the quantum structure of the theory, making their appearance as higher order corrections. It is there that the semileptonic B decays belong. The QCD corrections bring about a change of the decay rate of up to 20%, so it is important to take them into account in any description aspiring to realism.

This paper is concerned with making some progress towards the determination of some of the SM parameters by calculating QCD corrections to semileptonic B decays, which serve as the field of many tests of the model and are currently under heavy experimental investigation. Before reviewing the methods and previous results, let us delineate the objectives of these calculations.

One of them is the determination of the V_{ub} matrix element. The entries of the CKM matrix are of great import for the understanding of the physics behind the weak processes and theories have been proposed to disentangle the observed structure [23, 24, 25, 26]. If the matrix one day proves not to be unitary, which assertion would require precision measurements, it will be an undeniable sign of the existence of hitherto unknown species of particles. A more tangible problem related to these elements is the CP violation. It is due to none other than precise measurements [27, 28] that we now know that CP is directly violated. The value of V_{ub} has always been deducted from semileptonic B decays and we propose a way to establish it up to an uncertainty of 10%.

Our effort went also into finding the corrections to the polarisation of the τ lepton produced in B decays. Polarisation is a quantity blessed, a least potentially, with a smaller dependence on parameters compared to total rates. This is gorgeously shown in the case of the longitudinal polarisation of the charged lepton: even though the rate gets corrected by a fifth of its tree level value,

the polarisation is never affected by more than one percent. Such a quantity is an excellent candidate for determining the quark masses. These masses have been notorious for their haziness but the difference between the beautiful and charmed quarks is rather well defined. On the other hand, making predictions on absolute rates involves the masses themselves and is rather problematic. We will have more to say about that in the discussion of nonperturbative corrections.

Since we are unable to perform an exact calculation of the semileptonic decay rate (or any, for that matter), we must resort to some approximation or other. The zeroth order approximation results in the Born term. This is supplemented by corrections which can be divided into perturbative and nonperturbative. The perturbative ones are valid as long as the decaying particle can be viewed as almost free. Such an assumption is viable in B decay processes because of the high momenta transferred and the asymptotic freedom of partons in QCD. As mentioned above, the ensuing corrections are substantial and their inclusion is a must for an accurate prediction. The technique employed in these calculation is that of Feynman diagrams. The accuracy achieved in such a way can be estimated by looking at the relative size of some higher order quantities or at the various scale prescriptions giving what they claim to be the optimal value of the gauge coupling. Unfortunately, the evidence is not uplifting for B decays. The total rate gets a two loop correction of a size comparable to that of the one loop one, and the scale predicted by BLM scheme [29] is rather low, too.

At the same time, use has been made of the natural small parameter available in the description of the B decays, which is the ratio of the QCD scale to the released energy, the latter of the order of the b quark mass. The methods exploiting this fact are known as nonperturbative. The early phenomenological approach to explicitly deal with B decays was proposed by Altarelli et al. [30], who considered the probability of the b quark inside the meson to have a given kinetic energy as a function of this energy. The decay was to be calculated incoherently, which is plausible due to the large energy released during decay. This attempt, referred to as ACCMM, was later criticised by the proponents of the heavy quark effective theory, HQET, as failing to capture QCD-specific features of the decay process. HQET was developed [31] as a systematic expansion in terms of phenomenological parameters of the order of inverse quark mass. Later on, another type of expansion appeared [22], with the first nontrivial term corresponding to the leading twist approximation as used in deep inelastic scattering. The latter method emerged after the realisation of the difficulties that the mass expansion had had. In the end, the discrepancy between the phenomenological method and HQET has been seen diminishing. In our calculations we employ the HQET methods, but we take an interesting look at the kinematics of the process, using a generalised ACCMM model. Neither method is too illuminating about the mass of the quark in question. In HQET, the mass expansion can be challenged by questioning the notion of quark mass as a physical quantity. In ACCMM, this problem is even less well defined because of the arbitrary character of the incoherent integration. Of course we have to make specific predictions so we will state our assumptions clearly in Sec.5.

Our work is a continuation of the research done in this field. The semileptonic decays of B mesons have been investigated for some time using both perturbative and nonperturbative methods. As regards the total decay rate, the analogy to muon decay made it possible to use the old results [8], which were based on the calculation of radiative corrections performed in [7]. The $\mathcal{O}(\alpha_s)$ corrections to the lepton spectra were first given in a correct, analytical form in [32] (while numerical estimates were given in [33]) and then distributions taking into account the b quark polarisation were found [34]. The lepton mass was taken into account in [35, 36, 37], allowing to consider semitauonic decays. In [35], the one-loop order correction was also found to the longitudinal polarisation of the τ lepton in the rest frame of the virtual W boson. The polarisation turned out to be only slightly affected by the radiative corrections. We have found the analytic formulae for the longitudinal polarisation in the rest frame of the decaying quark in an analytic form, which is presented in this paper.

At the same time, the non-perturbative corrections were calculated. As the heavy quark effective theory arose together with the application of the operator product expansion, inclusive lepton spectra were considered, first in [31]. The calculation of the average hadronic mass squared discussed in that paper already suggested that the expansion in inverse powers of the decaying quark mass may start with the quadratic, rather than linear, terms. This statement, which in fact needed to be qualified and is now known as Luke's theorem [38], is true for the inclusive leptonic spectra, as is seen in particular from the results presented here. The actual non-trivial HQET corrections to the leptonic spectra were first found in [39] and the work was then extended to double differential spectra in electron energy and leptonic invariant mass squared [40, 41]. All these results neglected the mass of the final charged lepton. The latter was considered in [42, 43, 44], where the inclusive lepton spectra were calculated. In [45], the longitudinal polarisation of the τ lepton was found through order $1/m_b^2$. We apply the inverse mass expansion to evaluating the nonperturbative corrections to the polarisation of the tau lepton with respect to the momentum of the virtual W boson. The latter is advantageous from the experimental point of view [46, 47]. This HQET calculation shows some apparent divergencies, which however cancel. A similar, although different, problem was addressed in [48].

The determination of the V_{ub} matrix element is also about finding the perturbative and nonperturbative corrections. We have already mentioned the basic papers [8, 7, 32] concerning the perturbative part. On the other hand, the HQET provided the inverse mass expansions [31, 39, 40, 41]. However, it was clear from the beginning [39] that this kind of expansion suffers from singularities close to the high endpoint of the lepton energy spectrum. Usually this problem may be partially solved by resorting to moments. However, in the case of the charmless decays, it is exactly this part of the spectrum that is cleanly distinguishable from the much more copious charmed decays and therefore we would rather it were treatable on a more detailed basis. One method designed to sidestep these difficulties was the so-called leading twist expansion. We take this approach and propose a quantity that will enable measuring V_{ub} with an accuracy of 10%.

This dissertation comprises several results regarding the polarisation in semileptonic B decays and the determination of the V_{ub} matrix element. Apart from the leading twist convolution of the $b \rightarrow ue\bar{\nu}_e$ rate, these results have been published before. The one-loop QCD correction to the longitudinal τ polarisation has been published in [49]. The paper [50] contains the Born term of the polarisation of the τ lepton with respect to the momentum of the virtual W boson, while the $\mathcal{O}(m_b^2)$ corrections to it have been calculated in [51]. Lastly, the double differential distribution in terms of the hadronic mass and electron energy has been found through one loop order in [52].

The paper is organised as following. We start with the kinematics of the considered processes, in Sec.2. Then we discuss the types of corrections involved in the calculation, Sec. 3. At the end of that section, we devote some space to the discussion of the Fermi motion inside a B meson. In Sec. 4 we present the one loop correction to the double distribution in hadronic mass and electron energy. Sec. 5 is devoted to the discussion of this quantity in the context of measuring V_{ub} . It presents results taking into account the leading twist corrections. The polarisation of the τ lepton in $B \rightarrow X_c \tau \bar{\nu}_\tau$ decays is considered in Secs.6 and 7. First, we give the one loop corrections to the longitudinal polarisation and then, in Sec. 7, the nonperturbative corrections to the polarisation with respect to the momentum of the virtual W boson are given in an analytic form, while the inclusion of the corresponding perturbative contribution is performed numerically.

2 Kinematics

In this section, we wish to exhaust all the kinematic information about the processes that are going to be discussed further on. Except for the calculation of the $\mathcal{O}(1/m_b^2)$ corrections to the polarisation of the τ (see Sec.7), the results presented below are found in the rest frame of the decaying b quark. While this is rather obvious for the perturbative corrections, the leading twist corrections which are used also assume a static quark. The Fermi motion is reflected solely in the variable effective mass of the quark. One notes, moreover, that even the inverse mass expansion leads ultimately to kinematical ranges identical to the partonic ones.

2.1 Variables

The four-momenta of the particles are denoted as following:

- Q for the decaying quark,
- q for the final quark (charm or up),
- l for the charged lepton, or
- τ specifically for the τ lepton,
- ν for the antineutrino, and
- G for the final real gluon.

The system of the final quark and gluon has its momentum denoted as $P = q + G$, while the leptonic momentum is written as $W = l + \nu$. Then the scaled masses of the final particles are written in terms of the parameters defined as

$$\eta = \frac{\tau^2}{m_b^2}, \quad \rho \equiv \epsilon^2 = \frac{q^2}{m_b^2}. \quad (1)$$

The particles are assumed to be on shell. The following scaled variables have been employed in the partonic part of the calculations:

$$x = \frac{2v \cdot l}{m_b}, \quad t = \frac{(l + \nu)^2}{m_b^2}, \quad z = \frac{(q + G)^2}{m_b^2}, \quad x_p = \frac{2v \cdot P}{m_b}, \quad (2)$$

where v stands for the B meson four-velocity in its rest frame. For the perturbative calculation, the rest frame of the meson and the b quark coincide and then one can write,

$$x = \frac{2(Q \cdot l)}{m_b^2}, \quad t = \frac{(l + \nu)^2}{m_b^2}, \quad z = \frac{(q + G)^2}{m_b^2}, \quad x_p = \frac{2Q \cdot P}{m_b^2} \quad (3)$$

where x stands for the charged lepton energy, t for the invariant leptonic mass, z for the hadronic mass, and x_p for the hadronic energy, all scaled to the units of b quark mass. We also define the scaled neutrino energy, x_ν , but we reserve this symbol for the energy in the B meson rest frame. Denoting the meson four-velocity as v , we have

$$x_\nu = \frac{2v \cdot \nu}{m_b^2}. \quad (4)$$

The charged lepton is described by the light-cone variables:

$$\tau_{\pm} = \frac{1}{2}(x \pm \sqrt{x^2 - 4\eta}). \quad (5)$$

Thus, the system of the c quark and the real gluon is described by the following quantities:

$$P_0 = \frac{1}{2}(1 - t + z) \quad (6)$$

$$P_3 = \sqrt{P_0^2 - z} = \frac{1}{2}[1 + t^2 + z^2 - 2(t + z + tz)]^{\frac{1}{2}}, \quad (7)$$

$$P_{\pm}(z) = P_0(z) \pm P_3(z), \quad (8)$$

$$\mathcal{Y}_p = \frac{1}{2} \ln \frac{P_+(z)}{P_-(z)} = \ln \frac{P_+(z)}{\sqrt{z}} \quad (9)$$

where $P_0(z)$ and $P_3(z)$ are the energy and the length of the momentum vector of the system in the b quark rest frame, $\mathcal{Y}_p(z)$ is the corresponding rapidity. Similarly for the virtual boson W :

$$W_0(z) = \frac{1}{2}(1 + t - z), \quad (10)$$

$$W_3(z) = \sqrt{W_0^2 - t} = \frac{1}{2}[1 + t^2 + z^2 - 2(t + z + tz)]^{1/2}, \quad (11)$$

$$W_{\pm}(z) = W_0(z) \pm W_3(z), \quad (12)$$

$$\mathcal{Y}_w(z) = \frac{1}{2} \ln \frac{W_+(z)}{W_-(z)} = \ln \frac{W_+(z)}{\sqrt{t}}. \quad (13)$$

Kinematically, the three body decay is a special case of the four body one, with the four-momentum of the gluon set to zero, thus resulting in simply replacing $z = \rho$. The following variables are then useful:

$$p_0 = P_0(\rho) = \frac{1}{2}(1 - t + \rho) \quad , \quad p_3 = P_3(\rho) = \sqrt{p_0^2 - \rho}, \quad (14)$$

$$p_{\pm} = P_{\pm}(\rho) = p_0 \pm p_3 \quad , \quad w_{\pm} = W_{\pm}(\rho) = 1 - p_{\mp}, \quad (15)$$

$$Y_p = \mathcal{Y}_p(\rho) = \frac{1}{2} \ln \frac{p_+}{p_-} \quad , \quad Y_w = \mathcal{Y}_w(\rho) = \frac{1}{2} \ln \frac{w_+}{w_-}. \quad (16)$$

We also express the scalar products in terms of the variables used above, so in the units of the b quark mass one gets:

$$\begin{aligned} Q \cdot P &= \frac{1}{2}(1 + z - t) \quad , \quad \tau \cdot \nu = \frac{1}{2}(t - \eta), \\ Q \cdot \nu &= \frac{1}{2}(1 - z - x + t) \quad , \quad \tau \cdot P = \frac{1}{2}(x - t - \eta), \\ Q \cdot \tau &= \frac{1}{2}x \quad , \quad \nu \cdot q = \frac{1}{2}(1 - x - z + \eta). \end{aligned} \quad (17)$$

2.2 Kinematic boundaries

The boundaries of the kinematic variables depend on the process which we are dealing with. For the partonic part, one can distinguish between three and four body final states, the latter including a real gluon. A still different set of limits is obtained if one allows for Fermi motion, so that the hadronic entities enter the game. This motion is taken into account in the computation of the $\mathcal{O}(1/m_b^2)$ and leading twist corrections within the heavy quark effective theory. It is worth noting that these expansions have the net effect of formally leaving the b quark static.

2.2.1 Partonic limits

The scaled electron energy x can vary within the limits

$$2\sqrt{\eta} \leq x \leq 1. \quad (18)$$

With a fixed value of x , the limits of t are

$$\eta \leq t \leq \tau_+(1 - \frac{\rho}{1 - \tau_+}) \equiv t_2. \quad (19)$$

However, for the case of a final charm quark this range is conveniently split into two regions. In one of them, which we call A , both three-body and four-body processes are allowed, while in the other, B , only four-body final states are possible. The region A is delimited by

$$t_1 \equiv \tau_-(1 - \frac{\rho}{1 - \tau_-}) \leq t \leq t_2, \quad (20)$$

so that the remaining room of the phase space, B , corresponds to

$$\eta \leq t \leq t_1. \quad (21)$$

Conversely, if x should vary at a fixed value of t , the boundaries read:

$$\eta \leq t \leq (1 - \sqrt{\rho})^2, \quad w_- + \frac{\eta}{w_-} \leq x \leq w_+ + \frac{\eta}{w_+}, \quad (22)$$

for region A , and

$$\eta \leq t \leq \sqrt{\eta}(1 - \frac{\rho}{1 - \sqrt{\eta}}), \quad 2\sqrt{\eta} \leq x \leq w_- + \frac{\eta}{w_-}. \quad (23)$$

for region B . The upper limit of the mass squared of the final hadronic system is in both regions given by

$$z_{max} = (1 - \tau_+)(1 - t/\tau_+), \quad (24)$$

whereas the lower limit depends on the region:

$$z_{min} = \begin{cases} \rho & \text{in Region A} \\ (1 - \tau_-)(1 - t/\tau_-) & \text{in Region B} \end{cases} \quad (25)$$

2.2.2 Partonic limits - massless case

For the $b \rightarrow ue\bar{\nu}_e$ decay, the masses of the final particles may be treated as vanishing. Then the above kinematic limits simplify considerably. The electron energy x varies within the range of

$$0 \leq x \leq 1, \quad (26)$$

and for a fixed x , the invariant mass of hadrons can be

$$0 \leq z \leq 1 - x. \quad (27)$$

If we fix z first, it can take on values from

$$0 \leq z \leq 1, \quad (28)$$

and then the limits on x are

$$0 \leq x \leq 1 - z. \quad (29)$$

We will also use a triple distribution in terms of electron energy x , hadronic energy x_p and hadronic invariant mass z . With a fixed value of x ,

$$1 - x \leq x_p \leq 2 - x, \quad \max\{0, x_p - 1\} \leq z \leq (1 - x)(x_p + x - 1). \quad (30)$$

As mentioned above, for massless final particles, the distinction between the region where only four body final state is allowed and the rest disappears when speaking in terms of variables x, t, z fixed in this order. However, with the hadronic energy x_p used as a variable, an analogous division holds. It is now reflected in the fact that the values of $x_p > 1$ correspond to four-body final state.

2.2.3 Meson kinematic boundaries

In the evaluation of the $\mathcal{O}(1/m_b^2)$ corrections, it is necessary to work out the kinematics in the rest frame of the decaying meson. Let us denote the four-velocity of the decaying quark by v . The neutrino energy is no longer fixed by the other variables, as it is in the partonic calculation. Rather, it becomes another kinematic variable, see [42] for the boundaries. The partonic value of the neutrino energy is given by the relation

$$x_{\nu 0} = 1 + t - x - \rho. \quad (31)$$

3 Evaluation of corrections

3.1 Perturbative corrections

Let us denote the final c or u quark generically as q and the charged lepton as l . The QCD-corrected differential rate for the $b \rightarrow q + l_- + \bar{\nu}_l$ reads:

$$d\Gamma^\pm = d\Gamma_0^\pm + d\Gamma_{1,3}^\pm + d\Gamma_{1,4}^\pm, \quad (32)$$

where

$$d\Gamma_0^\pm = G_F^2 m_b^5 |V_{CKM}|^2 \mathcal{M}_{0,3}^\pm d\mathcal{R}_3(Q; q, \tau, \nu) / \pi^5 \quad (33)$$

is the Born approximation, while

$$d\Gamma_{1,3}^\pm = \frac{2}{3} \alpha_s G_F^2 m_b^5 |V_{CKM}|^2 \mathcal{M}_{1,3}^\pm d\mathcal{R}_3(Q; q, \tau, \nu) / \pi^6 \quad (34)$$

comes from the interference between the virtual gluon and Born amplitudes. Then,

$$d\Gamma_{1,4}^\pm = \frac{2}{3} \alpha_s G_F^2 m_b^5 |V_{CKM}|^2 \mathcal{M}_{1,4}^\pm d\mathcal{R}_4(Q; q, G, \tau, \nu) / \pi^7 \quad (35)$$

is due to the real gluon emission, G denoting the gluon four-momentum. V_{CKM} is the Cabibbo-Kobayashi-Maskawa matrix element corresponding to the b to c or u quark weak transition. The Lorentz invariant n -body phase space is defined as

$$d\mathcal{R}_n(P; p_1, \dots, p_n) = \delta^{(4)}(P - \sum p_i) \prod_i \frac{d^3 \mathbf{p}_i}{2E_i}. \quad (36)$$

The superscript \pm refers to the polarisation of the charged lepton when it is taken into account.

The three-body phase space is parametrized by Dalitz variables:

$$d\mathcal{R}_3(Q; q, \tau, \nu) = \frac{\pi^2}{4} dx dt. \quad (37)$$

To be specific, consider the unpolarised rates. The evaluation of the virtual gluon exchange matrix element yields:

$$\begin{aligned} \mathcal{M}_{1,3}^{un}(\tau) = & -[H_0 q \cdot \tau Q \cdot \nu + H_+ \rho Q \cdot \nu Q \cdot \tau + H_- q \cdot \nu q \cdot \tau \\ & + \frac{1}{2} \rho (H_+ + H_-) \nu \cdot \tau + \frac{1}{2} \rho (H_+ - H_- + H_L) [\tau \cdot (Q - q - \nu)] (Q \cdot \nu) \\ & - \frac{1}{2} H_L [\tau \cdot (Q - q - \nu)] (q \cdot \nu)] \end{aligned} \quad (38)$$

where

$$\begin{aligned} H_0 = & 4(1 - Y_p p_0 / p_3) \ln \lambda_G + (2p_0 / p_3) [Li_2(1 - \frac{p_- w_-}{p_+ w_+}) \\ & - Li_2(1 - \frac{w_-}{w_+}) - Y_p (Y_p + 1) + 2(\ln \sqrt{\rho} + Y_p) (Y_w + Y_p)] \end{aligned}$$

$$+[2p_3Y_p + (1 - \rho - 2t) \ln \sqrt{\rho}] / t + 4, \quad (39)$$

$$H_{\pm} = \frac{1}{2} [1 \pm (1 - \rho) / t] Y_p / p_3 \pm \frac{1}{t} \ln \sqrt{\rho}, \quad (40)$$

$$H_L = \frac{1}{t} (1 - \ln \sqrt{\rho}) + \frac{1 - \rho}{t^2} \ln \sqrt{\rho} + \frac{2}{t^2} Y_p p_3 + \frac{\rho}{t} \frac{Y_p}{p_3}, \quad (41)$$

and the superscript "un" stands for the unpolarised rate. After renormalization, the virtual correction $\mathcal{M}_{1,3}^{un}$ is ultraviolet convergent. However, the infrared divergences are left. They are regularized by a small mass of gluon denoted as λ_G . In accordance with the Kinoshita-Lee-Nauenberg theorem [10, 11], this divergence cancels out when the real emission is taken into account. The rate from real gluon emission is evaluated by integrating the expression

$$\mathcal{M}_{1,4}^{un}(\tau) = \frac{\mathcal{B}_1(\tau)}{(Q \cdot G)^2} - \frac{\mathcal{B}_2(\tau)}{Q \cdot G P \cdot G} + \frac{\mathcal{B}_3(\tau)}{(P \cdot G)^2}, \quad (42)$$

where

$$\mathcal{B}_1(\tau) = q \cdot \tau [Q \cdot \nu (Q \cdot G - 1) + G \cdot \nu - Q \cdot \nu Q \cdot G], \quad (43)$$

$$\begin{aligned} \mathcal{B}_2(\tau) = q \cdot \tau [G \cdot \nu - q \cdot \nu Q \cdot G + Q \cdot \nu (q \cdot G - Q \cdot G - 2q \cdot Q)] \\ + Q \cdot \nu (Q \cdot \tau q \cdot G - G \cdot \tau q \cdot Q), \end{aligned} \quad (44)$$

$$\mathcal{B}_3(\tau) = Q \cdot \nu (G \cdot \tau q \cdot G - \rho \tau \cdot P). \quad (45)$$

The polarized case requires an appropriate substitution of the lepton four-momentum τ present in the formulae above by a combination of four-momenta specific for a sought polarisation. The expressions defining these relations are given in the following sections. It will also be seen that this is true both for the Born approximation and the corrections affecting the hadronic tensor.

The four-body phase space is decomposed as follows:

$$d\mathcal{R}_4(Q; q, G, \tau, \nu) = dz d\mathcal{R}_3(Q; P, \tau, \nu) d\mathcal{R}_2(P; q, G). \quad (46)$$

After employing the Dalitz parametrization of the three body phase space \mathcal{R}_3 and integration we arrive at an infrared-divergent expression.

The method used in these calculations is the same as the one employed in the previous ones [36, 37, 32, 53]. The infrared-divergent part is regularized by a small gluon mass λ_G which enters into the expressions as $\ln(\lambda_G)$. When the three- and four-body contributions are added the divergent terms cancel out and then the limit $\lambda_G \rightarrow 0$ is performed. This procedure yields well-defined double-differential distributions of lepton spectra as described in the following sections.

3.2 Nonperturbative corrections

The b quark is confined within a B meson so its decay cannot be completely described if one sticks with the perturbative, partonic picture where the quark

is treated as an almost free particle. While the large momentum transfer accompanying the decay renders it suitable for such an analysis in a theory that is asymptotically free, some effects remain and have to be addressed via non-perturbative techniques. The HQET methods have established their status as *the* tool to deal with semileptonic B decays and we are using them here. They provide a systematic expansion around the limit of infinite quark masses, where new symmetries arise, those of flavour and of spin. The expansion comes in two kinds. It can be done in terms of consequent orders of the inverse mass of the decaying quark, or according to the twist of the operators included.

3.2.1 Corrections of order $1/m_b^2$

Using the operator expansion technique, one can obtain corrections to the decay widths of heavy hadrons which effectively lead to new terms in the hadronic tensor appearing in the triple differential decay width,

$$\frac{d\Gamma}{dx_\nu dt dx} = \frac{|V_{cb}|^2 G_F^2}{2\pi^3} \mathcal{L}_{\mu\nu} \mathcal{W}_{\mu\nu} \quad . \quad (47)$$

The hadronic tensor \mathcal{W} , related to an inclusive decay of a beautiful hadron H_b ,

$$\mathcal{W}_{\mu\nu} = (2\pi)^3 \sum_X \delta^4(p_{H_b} - q - p_X) \langle H_b(v, s) | J_\mu^{c\dagger} | X \rangle \langle X | J_\nu^c | H_b(v, s) \rangle \quad (48)$$

can be expanded in the form

$$\mathcal{W}_{\mu\nu} = -g_{\mu\nu} W_1 + v_\mu v_\nu W_2 - i\epsilon_{\mu\nu\alpha\beta} v^\alpha q^\beta W_3 + q_\mu q_\nu W_4 + (q_\mu v_\nu + v_\mu q_\nu) W_5 \quad . \quad (49)$$

The form factors W_n can be determined by using the relation between the tensor \mathcal{W} and the matrix element of the transition operator

$$T_{\mu\nu} = -i \int d^4x e^{-iqx} T[J_\mu^{c\dagger}(x) J_\nu^c(0)] \quad , \quad (50)$$

which is

$$\mathcal{W}_{\mu\nu} = -\frac{1}{\pi} \text{Im} \langle H_b | T_{\mu\nu} | H_b \rangle \quad . \quad (51)$$

The coefficients W_n of (49) have all been found elsewhere, see eg. [42] for a complete list. Then the distribution (47) can be schematically cast in the following form:

$$\frac{d\Gamma}{dx_\nu dt dx} = f_1 \delta(x_\nu - x_{\nu 0}) + f_2 \delta'(x_\nu - x_{\nu 0}) + f_3 \delta''(x_\nu - x_{\nu 0}) \quad , \quad (52)$$

where

$$x_{\nu 0} = 1 + t - \rho - x \quad (53)$$

is the value of the neutrino energy in the parton model kinematics. The triple differential distribution must be integrated over the neutrino energy to give

meaningful results. The final lepton energy distribution obtained on two subsequent integrations may be trusted except for the endpoint region where the operator product expansion fails. In the present paper we give the double differential distribution so that the lepton energy distribution has to be obtained numerically. The calculation does not show any features unfamiliar from the cases of the other known polarisations, although apparent divergences pop up.

3.2.2 Leading twist approximation

In certain kinematical regions, the inverse mass expansion does not work due to the fact that the formally higher terms do not get smaller. Then it may still be possible to perform an expansion in terms of increasing twist of the retained operators. This technique is taken over from the deep inelastic scattering methods. It is applicable when the assumption is valid that the four-momentum of the final state hadrons is almost light-like. This is the large momentum that has to occur in a twist expansion.

Under that assumption, the generic quantity Γ characterizing the B decay can be written as

$$\Gamma(\Xi_i) = \int dk_+ f(k_+) \Gamma^{partonic}(\xi_i) \delta[\Xi(\xi)]. \quad (54)$$

In the above formula, $\Gamma^{partonic}$ is the sought quantity as evaluated within the parton model with the b quark mass set to $m_b + k_+ \equiv m_b^*$. The variables characterizing the partonic system are generically denoted as ξ while those corresponding to the hadronic system by Ξ . The relation between the hadron and parton system variables involves kinematics in which the b quark is viewed as static but has a variable effective mass m_b^* . Thus the expression has the form of a convolution of the partonic rate with the so-called *shape function* $f(k_+)$. This function is a nonperturbative entity, defined as

$$f(k_+) = \langle B | b \delta(D_+ - k_+) \bar{b} | B \rangle, \quad (55)$$

with D_+ defining the light-cone component of the covariant derivative.

In the expression (54) the partonic rate is evaluated for a quark mass equal m_b^* , but this replacement is not made everywhere. The prefactor m_b^5 is left constant. We will not discuss this prescription, although it seems admittedly *ad hoc*. Let us just note that in the ratio of decay rates, which is what we study, this point may be believed not to cause too much trouble.

3.2.3 Discussion of Fermi motion

In this paper, what we use are the perturbative corrections and the HQET methods of including Fermi motion effects. The latter are worth discussing for a while. When it comes to differential spectra, the leading twist approximation is the realistic way of using heavy quark theory. In this approximation, the dependence of the kinematics on the Fermi motion is rather formal, with the quark effectively staying at rest and having a variable mass. We therefore think

it an interesting point to make to consider the kinematics of the Fermi motion from a general point of view. Even though we abandon the leading twist approximation and the kinematic conditions it depends upon, we are still led to non-trivial conclusions.

The products of the decay, the hadronic system and the two leptons, can be characterised by three variables, which one may choose to be the hadronic invariant mass squared M_X^2 and the energies of each lepton, E_l for the electron and E_ν for the neutrino. The neutrino energy can be measured indirectly using energy-momentum conservation. The task of including the Fermi motion consists in performing a boost from the rest frame of the b quark to that of the decaying meson. Then one can sum incoherently over the various configurations of the quark in the meson. This probabilistic approach is based on the fact that the momentum transfer in the decay is large enough to make an impulse approximation valid. We will thus relate the above introduced variables to the ones defined in the b quark rest frame. Quantities in this frame will be denoted with an asterisk: P^* for the partonic four-momentum, E_l^* and E_ν^* for the lepton energies. Because of the form of the distribution formulae, it is convenient to also employ the scaled variables,

$$x_l = \frac{2E_l^*}{m_b}, \quad x_\nu = \frac{2E_\nu^*}{m_b}, \quad z = \frac{P^2}{m_b^2}. \quad (56)$$

In the above definition, the mass m_b of the b quark will in general vary as it is the effective quark mass which defines the kinematics of the process. However, we will not vary the factor of m_b^5 multiplying the decay width since this factor, reflecting the phase space suppression, is probably compensated for by the Coulomb enhancement. As a matter of fact, this mass dependence will drop out of the ratio of the charmless to charmed decays.

In order to specify the relation between the two frames of interest, one needs to parametrise the Fermi motion. We do this in a general way, making no assumptions on the specific form of the distribution of the quark or the light degrees of freedom.

Working in the rest frame of the B meson, assume that the heavy quark has three-momentum \vec{k} and energy E_b . Forming a bound state, the quark is generally off mass shell and its effective mass is then $\mu = \sqrt{E_b^2 - |\vec{k}|^2}$. Neither are the light degrees of freedom assumed to have the mass of the light quark. In fact, using energy and momentum conservation, we write the four-momentum K of the spectator as

$$K = (M_B - E_b, -\vec{k}) \equiv (E_s, -\vec{k}). \quad (57)$$

Then we have set up the framework for performing the boost. Starting from the system where the b quark stays at rest, the boost needs to endow it with momentum \vec{k} , which defines its parameters to be

$$\gamma = \frac{E_b}{\mu} \quad \text{and} \quad \vec{\beta} = \frac{\vec{k}}{E_b}. \quad (58)$$

It is instructive to look closely at the transformation formulae for the different quantities. The electron energy in the B meson frame can be written as

$$E_l = \frac{1}{2}x_l(M_B - E_s + |\vec{k}| \cos \theta_l) \quad (59)$$

where θ_l is the angle between the directions of the electron and the momentum \vec{k} . Similarly, the neutrino energy is transformed according to the formula

$$E_\nu = \frac{1}{2}x_\nu(M_B - E_s + |\vec{k}| \cos \theta_\nu) \quad (60)$$

with θ_ν denoting the corresponding angle for the neutrino. Note that in each of Eqs.(59,60) the reference to the Fermi motion is encoded in one rather than two variables. These are, respectively for the electron and neutrino,

$$k_{l,+} \equiv E_s - |\vec{k}| \cos \theta_l, \quad \text{and} \quad k_{\nu,+} \equiv E_s - |\vec{k}| \cos \theta_\nu. \quad (61)$$

It is easy to verify that this structure is due to the fact that the corresponding particles are massless. The other case is relevant for the lepton pair, which usually has a non-vanishing invariant mass, yielding the following relation between the B meson energy, E_W , and the scaled energy in the quark rest frame,

$$x_W = \frac{1}{2}(x_l + x_\nu) = \frac{E_W}{\mu}, \quad (62)$$

$$E_W = M_B x_W - E_s x_W - |\vec{k}| \cos \theta_W \sqrt{(1 - x_W^2) - z}. \quad (63)$$

Clearly, different values of z make different combinations of E_s and $|\vec{k}| \cos \theta_W$ contribute to this expression. In the case of the massless leptons, therefore, we can reduce the Fermi motion dependence to a function of the variable $k_{X,+}$, X denoting a generic particle. This justifies the use of the convolution with the light-cone shape function. On the contrary, the invariant mass of the lepton system cannot be calculated in this way. It also obvious that the double differential spectrum of lepton energies also has a more general dependence since it involves two different combinations of $|\vec{k}|$ and E_s .

Let us now have a look at the energy spectrum of the hadron system. It might at first seem that as long as it can be viewed as massless the light-cone dominance is in effect. However, one realizes easily that this distribution is directly related to that of the W energy by the relation $M_B = E_W + E_H$, E_H standing for the hadronic energy in B meson rest frame. The arguments applied to massless leptons do not work here since the energy of the hadrons is the sum of the parton and spectator energy. The latter inevitably is disconnected from the boost and contributes pure energy rather than the required combination:

$$E_H = M_B x_H + E_s - x_H k_{+,H}. \quad (64)$$

For the hadronic invariant mass, the reduction fails to hold if this mass does not vanish:

$$M_X^2 = E_b^2 z + x_H E_b E_s + |\vec{p}_H| E_b |\vec{k}| \cos \theta_H + \mathcal{O}(|\vec{k}|^2). \quad (65)$$

4 Spectrum of hadronic mass and electron energy

4.1 Introduction

The spectrum of hadronic mass and electron energy is a quantity that can be helpful in extracting the V_{ub} matrix element. This section shows the perturbative corrections to this distribution which are essential due to their numerical value of approximately 20%. We will later on take a more comprehensive approach at the spectrum of hadron mass and electron energy, but this partonic distribution can be useful to let us see clearly what effects come from non-perturbative regime and is also evidently a check on the more sophisticated calculations. Moreover, while the more realistic calculations rely on modelling in one way or another, moments of distributions are believed to be correctly given by partonic results due to parton-hadron duality.

We postpone the discussion of the current status of the $|V_{ub}|$ related calculations until the next section, where the leading twist approximation is discussed. Here, we present the way we evaluate the perturbative corrections in Subsection 4.2, then show the analytical results, Subsec. 4.3 and use them to evaluate a few moments of the hadronic mass distribution, Subsec. 4.4. The contents of this section has been published in [52].

4.2 Evaluation

The tree level result for this spectrum can be read off from the previously given formulae, while the one-loop corrections are evaluated following an analogous procedure. This calculation, however, required the evaluation of the integral over the three-body phase space of the vertex correction as well as the integration of the four-body decay rate.

As regards the virtual gluon contribution, integration over the invariant mass of the intermediate W boson gives the desired contribution to the double differential distribution,

$$\begin{aligned} \frac{d\Gamma_{1,3}}{12\Gamma_0 dx dz} = \delta(z) \{ & \frac{1}{3} \log \lambda_G [10x - 25x^2 + \frac{34}{3}x^3 + (10 - 24x + 18x^2 - 4x^3) \log \bar{x} \\ & - 6x^2 \log \epsilon + 4x^3 \log \epsilon] + \frac{1}{3}(2x^3 - 3x^2) \text{Li}_2(x) + \frac{1}{18} \log \bar{x} [121 \\ & - 276x + 195x^2 - 40x^3 - \log \bar{x} (30 - 72x + 54x^2 - 12x^3)] \\ & + \frac{121}{18}x - \frac{443}{36}x^2 + \frac{128}{27}x^3 + \frac{1}{6} \log \epsilon (-3x^2 + 2x^3 + 6x^2 \log \epsilon \\ & - 4x^3 \log \epsilon) \}, \end{aligned} \quad (66)$$

where we have denoted

$$\bar{x} = 1 - x. \quad (67)$$

While we present the decay rate assuming massless final particles, it is not possible to eliminate the final quark as well as gluon mass dependence out of

the matrix element alone. This is removed once the integrated real radiation term is added. This rate is conveniently split into terms according as they are infrared convergent or divergent. Hence we can write,

$$\frac{d\Gamma_{1,4}}{12\Gamma_0 dx dt dz} = \mathcal{F}_{conv} + \mathcal{F}_{div}. \quad (68)$$

Integration over t gives

$$\int_0^{t_m} \mathcal{F}_{div} dt = \mathcal{F}_{div,s}\delta(z) + \mathcal{F}_{div,c}\theta(z - \lambda_G^2), \quad (69)$$

and we obtain the following expressions for the above integral:

$$\begin{aligned} \mathcal{F}_{div,c} = & \log z [\bar{x}^{-1}(8z + 6z^2) + \bar{x}^{-2}(-z - 3z^2) + 2\bar{x}^{-3}z^2/3 \\ & + \log \bar{x}(16 - 4xz - 14x + 2x^2 + 18z + 2z^2) + 12xz + 16x - x^2/z \\ & - 7x^2 + \frac{2}{3}x^3/z - 7z - \frac{11}{3}z^2] \\ & + \log \bar{x} [\bar{x}^{-1}(-16z - 12z^2) + \bar{x}^{-2}(2z + 6z^2) - 4\bar{x}^{-3}z^2/3 \\ & + 22 - 8x/z - 12xz - 36x + 6x^2/z + 10x^2 - \frac{4}{3}x^3/z + \frac{10}{3}z^{-1} - 4z] \\ & + \log^2 \bar{x} (-16 + 4xz + 14x - 2x^2 - 18z - 2z^2) + \bar{x}^{-1}(-20z - 14z^2) \\ & + \bar{x}^{-2}(2z + 5z^2) - \frac{10}{9}\bar{x}^{-3}z^2 + \frac{10}{3}xz^{-1} - 2xz + 22x - \frac{22}{3}x^2z^{-1} \\ & - 9x^2 + \frac{28}{9}x^3z^{-1} + 18z + \frac{91}{9}z^2, \end{aligned} \quad (70)$$

$$\begin{aligned} \mathcal{F}_{div,s} = & -\frac{1}{9}\{9x^2\epsilon^2\log \lambda_G + \log \lambda_G[\log(1-x)](-30 + 72x - 54x^2 + 12x^3) \\ & + \log \lambda_G(-30x + 57x^2 - 22x^3) + \log \lambda_G \log \frac{\lambda_G}{\epsilon}(18x^2 - 12x^3) \\ & + \log \epsilon(1 + \log \epsilon)(9x^2 - 6x^3) + (-64 + 156x - 120x^2 + 28x^3)\log \bar{x} \\ & + (15 - 36x + 27x^2 - 6x^3)\log^2 \bar{x} - 64x + 3\pi^2x^2 + 100x^2 - 2\pi^2x^3 \\ & - 100x^3/3\}. \end{aligned} \quad (71)$$

The infrared finite part has been integrated with the help of FORM. It gives, in the same notation,

$$\int_0^{t_m} \mathcal{F}_{conv} dt = \mathcal{F}_{conv,s}\delta(z) + \mathcal{F}_{conv,c}\theta(z - \lambda_G^2), \quad (72)$$

with

$$\begin{aligned} \mathcal{F}_{conv,s} = & \log \lambda_G(-3x^2/2 + x^3) + \frac{1}{48}(173 - 360x + 240x^2 - 44x^3)\log \bar{x} \\ & + \frac{1}{8}(3x^2 - 2x^3)\log \epsilon + \frac{1}{96}(346x - 657x^2 + 294x^3), \end{aligned} \quad (73)$$

$$\begin{aligned}
\mathcal{F}_{conv,c} = & \log z (\bar{x}^{-1}(2z - 3z^2) + \bar{x}^{-2}z^2 + 9xz + 16x - 9x^2 - 2z + 2z^2) \\
& + \log \bar{x} [\bar{x}^{-1}(-4z + 6z^2) - 2z^2\bar{x}^{-2} + 57/2 - 5xz - 45x + 25x^2/2 \\
& - 27z - 3z^2/2] + \log \bar{x} \log \frac{\bar{x}}{z} (-16 + 2xz + 16x - 2x^2 - 11z + z^2) \\
& + 1/4 [\bar{x}^{-1}(-58z + 6z^2) + \bar{x}^{-2}(+3z + 5z^2) - 2z^2\bar{x}^{-3} - 72xz \\
& + 114x - 3x^2z^{-1} - 61x^2 + 2x^3z^{-1} + 55z - 9z^2]. \tag{74}
\end{aligned}$$

The formulae above suffer from infrared and collinear divergences. Thence the gluon and final quark masses subsist as regulators in spite of the limit we have taken. Of course, both remnant dependences vanish after the integration over the hadronic system mass is performed, which involves summing the virtual and real contributions. As a matter of fact, the part we have termed as convergent, given by Eq. (72), may be integrated on its own and then only the logarithm of the final quark mass still remains, reflecting the collinear divergence to be cancelled against a similar term in the virtual correction.

4.3 Analytical results

The first order QCD corrected double differential decay rate can be written in the form,

$$\frac{d\Gamma}{12\Gamma_0 dx dz} = f_0(x)\delta(z) + \frac{2\alpha_s}{3\pi} [f_1^s\delta(z) + f_1^c(x, z)\theta(z - \lambda_G^2)], \tag{75}$$

with

$$\Gamma_0 = \frac{G_F^2 m_b^5}{192\pi^3}, \tag{76}$$

where the first term on the right hand side is the Born approximation, given by

$$f_0(x) = \frac{1}{6}x^2(3 - 2x), \tag{77}$$

while

$$\begin{aligned}
f_1^s(x) = & -4f_0(x)\log^2 \lambda_G + \frac{1}{18}(120x - 291x^2 + 130x^3)\log \lambda_G \\
& + \frac{1}{3}(-10 + 24x - 18x^2 + 4x^3)\log \bar{x} \log \left(\frac{\bar{x}}{\lambda_G^2} \right) \\
& + \frac{1}{6}(83 - 196x + 145x^2 - 32x^3)\log \bar{x} \\
& + \frac{1}{18}(249x - 426x^2 + 155x^3) - \frac{2}{3}f_0(x) [\pi^2 + 3\text{Li}_2(x)], \tag{78}
\end{aligned}$$

and

$$\begin{aligned}
f_1^c(x, z) = & \frac{1}{z} [-2f_0(x)\log z + \frac{1}{36}(120x - 291x^2 + 130x^3) + \frac{1}{3}(10 - 24x \\
& + 18x^2 - 4x^3)\log \bar{x}] + [(10z + 3z^2)/\bar{x} - (z + 2z^2)/\bar{x}^2
\end{aligned}$$

$$\begin{aligned}
& + \frac{2}{3} z^2 / \bar{x}^3] \log \frac{z}{\bar{x}^2} + \frac{1}{2} \bar{x}^{-1} (-69z - 25z^2) + \frac{1}{4} \bar{x}^{-2} (11z + 25z^2) \\
& + \bar{x}^{-3} (-29z^2 / 18) + (101/2 - 17xz - 81x + 45x^2 / 2 \\
& - 31z - 3z^2 / 2) \log \bar{x} + (32 - 6xz - 30x + 4x^2 + 29z \\
& + z^2) \log \bar{x} \log \frac{z}{\bar{x}} + \log z (21xz + 32x - 16x^2 - 9z - 5z^2 / 3) \\
& - 20xz + 101x/2 - 97x^2/4 + 127z/4 + 283z^2/36. \tag{79}
\end{aligned}$$

The above formula is easily integrated over either of the variables to give the single differential distributions in hadronic system mass or charged lepton energy. Then expressions confirming previous calculations [32, 54, 55] are found. The evident singularity of this distribution disappears after integration over the hadronic system mass. That this indeed is so, can be seen by expressing it in terms of the following distributions,

$$\left(\frac{1}{z} \right)_+ = \lim_{\lambda \rightarrow 0} \left(\frac{1}{z} \theta(z - \lambda) + \log \lambda \delta(z) \right), \tag{80}$$

$$\left(\frac{\log z}{z} \right)_+ = \lim_{\lambda \rightarrow 0} \left(\frac{\log z}{z} \theta(z - \lambda) + \frac{1}{2} \log^2 \lambda \delta(z) \right). \tag{81}$$

The substitution of these to Eqs.(78,79) results in the formal identification,

$$\theta(z - \lambda_G^2) \frac{1}{z} = \theta(z - \lambda_G^2) \left(\frac{1}{z} \right)_+ - \delta(z) \log \lambda_G^2, \tag{82}$$

$$\theta(z - \lambda_G^2) \frac{\log z}{z} = \theta(z - \lambda_G^2) \left(\frac{\log z}{z} \right)_+ - \frac{1}{2} \log^2 \lambda_G^2 \delta(z). \tag{83}$$

Upon application of Eqs. (82,83) to the correction terms, the latter take on the following form:

$$\begin{aligned}
f_1^s(x) = & \frac{1}{3} (-10 + 24x - 18x^2 + 4x^3) \log^2 \bar{x} \\
& + \frac{1}{6} (83 - 196x + 145x^2 - 32x^3) \log \bar{x} \\
& + \frac{1}{18} (249x - 426x^2 + 155x^3) - \frac{2}{3} f_0(x) [\pi^2 + 3 \text{Li}_2(x)], \tag{84}
\end{aligned}$$

$$\begin{aligned}
f_1^c(x, z) = & -2f_0(x) \left(\frac{\log z}{z} \right)_+ + \left(\frac{1}{z} \right)_+ \left[\frac{1}{36} (120x - 291x^2 + 130x^3) \right. \\
& \left. + \left(\frac{10}{3} - 8x + 6x^2 - \frac{4}{3}x^3 \right) \log \bar{x} \right] + \left[(10z + 3z^2) / \bar{x} - (z + 2z^2) / \bar{x}^2 \right. \\
& \left. + \frac{2}{3} z^2 / \bar{x}^3 \right] \log \frac{z}{\bar{x}^2} + \frac{1}{2} \bar{x}^{-1} (-69z - 25z^2) + \frac{1}{4} \bar{x}^{-2} (11z + 25z^2) \\
& + \bar{x}^{-3} (-29z^2 / 18) + (101/2 - 17xz - 81x + 45x^2 / 2 \\
& - 31z - 3z^2 / 2) \log \bar{x} + (32 - 6xz - 30x + 4x^2 + 29z
\end{aligned}$$

$$+z^2) \log \bar{x} \log \frac{z}{\bar{x}}+\log z (21 x z+32 x-16 x^2-9 z-5 z^2/3) \\ -20 x z+101 x/2-97 x^2/4+127 z/4+283 z^2/36. \quad (85)$$

Clearly, the gluon mass does not enter the integrated distribution, defined as

$$F(x, z) = \frac{1}{12\Gamma_0} \int_0^z dz' \frac{d\Gamma}{dx dz'} = f_0(x) + \frac{2\alpha_s}{3\pi} F_1(x, z), \quad (86)$$

for which we obtain,

$$F_1(x, z) = (c_1 + c_2 z + c_3 z^2 + c_4 z^3) \log z + c_5 \log^2 z + c_6 z + c_7 z^2 + c_8 z^3 + c_9. \quad (87)$$

The coefficients c_1 to c_9 are as follows,

$$\begin{aligned} c_1 &= \frac{1}{36} [(120 - 288x + 216x^2 - 48x^3) \log \bar{x} + 120x - 291x^2 + 130x^3], \\ c_2 &= (-30x + 4x^2 + 32) \log \bar{x} + 32x - 16x^2, \\ c_3 &= 5\bar{x}^{-1} - \frac{1}{2}\bar{x}^{-2} + \frac{1}{2}(-6x + 29) \log \bar{x} + (21x - 9)/2, \\ c_4 &= \bar{x}^{-1} - \frac{2}{3}\bar{x}^{-2} + \frac{2}{9}\bar{x}^{-3} + \frac{1}{3} \log \bar{x} - 5/9, \\ c_5 &= -x^2/2 + x^3/3, \\ c_6 &= \frac{1}{2}(-102x + 37x^2 + 37) \log \bar{x} + (30x - 4x^2 - 32) \log^2 \bar{x} + \\ &\quad (74x - 33x^2)/4, \\ c_7 &= \frac{1}{4}(-28x - 91) \log \bar{x} + \frac{1}{2}(6x - 29) \log^2 \bar{x} - 10\bar{x}^{-1} \log \bar{x} - \frac{79}{4}\bar{x}^{-1} + \\ &\quad \bar{x}^{-2}(\log \bar{x} + \frac{13}{8}) - \frac{61}{4}x + \frac{145}{8}, \\ c_8 &= \frac{1}{36} \{ -22 \log \bar{x} - 12 \log^2 \bar{x} - 72\bar{x}^{-1} \log \bar{x} - 162\bar{x}^{-1} \\ &\quad + 48\bar{x}^{-2} \log \bar{x} + 83\bar{x}^{-2} - 16\bar{x}^{-3} \log \bar{x} - 22\bar{x}^{-3} + 101 \}, \\ c_9 &= \frac{1}{36} \{ 6(83 - 196x + 145x^2 - 32x^3) \log \bar{x} + 12(-10 + 24x \\ &\quad - 18x^2 + 4x^3) \log^2 \bar{x} - 12\pi^2 x^2 + 8\pi^2 x^3 + 498x \\ &\quad - 852x^2 + 310x^3 - 36x^2 \text{Li}_2(x) + 24x^3 \text{Li}_2(x) \}. \end{aligned} \quad (88)$$

4.4 Moments

One way of making comparison between the parton model predictions and the resonance ridden experimental data is to consider moments of distribution. We define those as

$$M_n(x) = \frac{1}{12\Gamma_0} \int_0^{1-x} z^n \frac{d\Gamma}{dx dz} dz. \quad (89)$$

While the zeroth moment corresponds to the electron energy distribution itself, the singular part of the double distribution leaves no trace on the higher moments. In fact, they are then vanishing in the Born approximation. The first five moments are expressed in terms of the following functions,

$$M_n(x) = \frac{2\alpha_s}{3\pi} m_n(x), \quad n \geq 1, \quad (90)$$

which are given by the formulae beneath (see also Fig. 1):

$$\begin{aligned} m_1 &= (-35/144 + 5x^2/8 - 4x^3/9 + x^4/16) \log \bar{x} \\ &\quad - 35x/144 + 19x^2/72 - x^3/48, \end{aligned} \quad (91)$$

$$\begin{aligned} m_2 &= (-449/3600 + 7x/24 - 61x^2/360 - 2x^3/45 + 13x^4/240 \\ &\quad - 13x^5/1800) \log \bar{x} - 449x/3600 + 533x^2/1800 - 9x^3/40 \\ &\quad + 109x^4/1800 - x^5/144, \end{aligned} \quad (92)$$

$$\begin{aligned} m_3 &= (-103/1800 + 119x/600 - 29x^2/120 + 19x^3/180 + x^4/120 \\ &\quad - 3x^5/200 + x^6/600) \log \bar{x} - 103x/1800 + 697x^2/3600 \\ &\quad - 653x^3/2700 + 49x^4/360 - 7x^5/200 + 47x^6/10800, \end{aligned} \quad (93)$$

$$\begin{aligned} m_4 &= \log \bar{x} (-1313/44100 + 2x/15 - 81x^2/350 + 59x^3/315 - 5x^4/84 \\ &\quad - x^5/175 + 2x^6/315 - 2x^7/3675) - 1313x/44100 + 5729x^2/44100 \\ &\quad - 11x^3/49 + 857x^4/4410 - 781x^5/8820 + 311x^6/14700 \\ &\quad - 19x^7/7350, \end{aligned} \quad (94)$$

$$\begin{aligned} m_5 &= \log \bar{x} (-485/28224 + 23x/245 - 211x^2/1008 + 151x^3/630 \\ &\quad - 95x^4/672 + 2x^5/63 + 29x^6/5040 - x^7/294 + 31x^8/141120) \\ &\quad - 485x/28224 + 1321x^2/14400 - 15879x^3/78400 \\ &\quad + 33599x^4/141120 - 4523x^5/28224 + 979x^6/15680 \\ &\quad - 9809x^7/705600 + 163x^8/100800. \end{aligned} \quad (95)$$

4.5 Summary

In this section we have presented the results from [52], where they were found for the first time. The analytical formulae have been shown for the double differential distribution in hadronic mass and electron energy in semileptonic B decays. These corrections can be meaningfully used on their own by calculating moments of the hadronic mass distributions, which we have presented, too. We will extend this study to a more specific method of determining $|V_{ub}|$ in the next section.

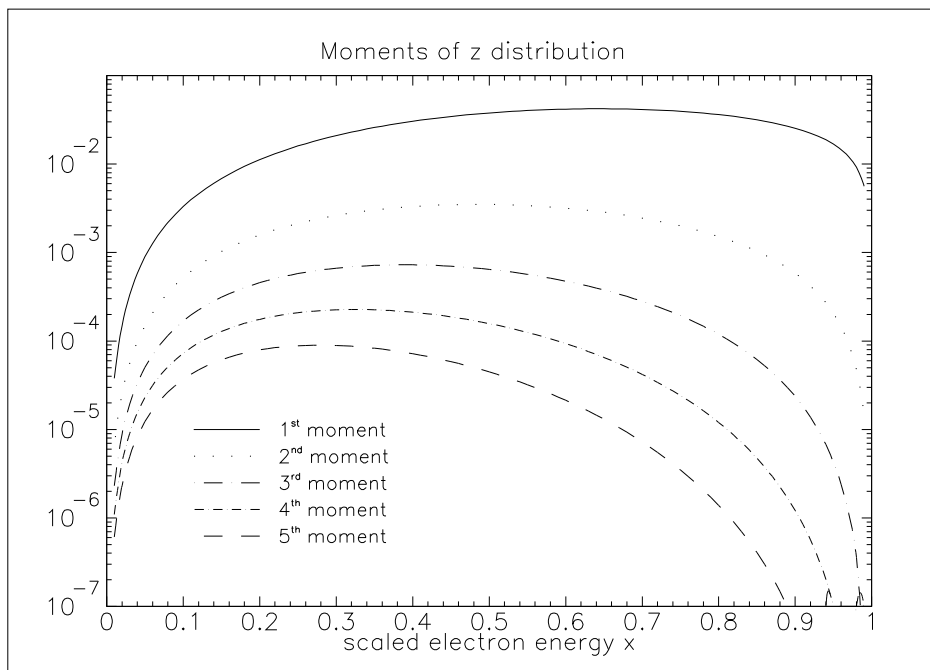


Figure 1: Moments of hadron mass distribution m_n as a function of the scaled electron energy x . The first five moments are shown as indicated by the legend.

5 Extraction of $|V_{ub}|$ from B decays

5.1 Introduction

The elements of the Cabibbo-Kobayashi-Maskawa mixing matrix are central to the physics of electroweak interactions. A precise determination of these is essential in establishing the unitarity of this matrix and so the completeness of the Standard Model, as well as in unveiling the nature of the CP violating interactions that remain puzzling. The beauty to up transition element, V_{ub} , is one of the smallest and least known of the matrix. The current PDG estimate ranges from $|V_{ub}| = 0.002$ to $|V_{ub}| = 0.005$. It is therefore currently a significant problem of particle physics to obtain a better estimate of it. As B factories are now under operation, the experimental data can be expected to offer greater accuracy so that theoretical prediction should also aim at a higher level of sophistication.

The V_{ub} matrix element has long been extracted from semileptonic B decays owing to their relative cleanliness. They are basically due to the weak interactions, but are affected by chromodynamical quantum corrections. The inclusion of the latter is vital due to their significant size of up to 20%. The process at hand has been studied using perturbative and nonperturbative techniques to take QCD effects into account. In our present case, QED calculations are of use [7] due to the topology of the diagrams involved. While the total decay rate of b to u can be inferred from an analogous analysis of the muon decay, due to Berman [8], numerical calculations of spectra appeared in [33], and the first correct analytical one-loop results were published in [32].

All of the calculations mentioned so far dealt with the perturbative corrections, which are valid due to the large momentum transfer occurring in the B decays. On the other hand, nonperturbative corrections are not negligible, but due to their relative smallness can be evaluated using an expansion in the scale provided by the ratio of the QCD scale to the transferred energy. A first, phenomenological approach was proposed in [30], where the b quark inside a meson was assigned a probability distribution describing its Fermi motion. The decay was then calculated on an incoherent basis. This method, referred to as ACCMM after the names of the article's authors, has later been dismissed by the proponents of a more systematic formulation, the heavy quark effective theory (HQET), as falling short of describing some aspects of the decays, allegedly accessible with HQET. With a systematic expansion proposed in [31], the new method was used to calculate the first nontrivial corrections [39] to lepton spectra. These corrections were expressed as an expansion in inverse powers of the heavy quark mass and involved terms viewed as breaking the heavy quark and spin symmetry, two symmetries of the effective lagrangian. Double differential spectra were considered in [41, 40] while the mass of the final lepton began to be included with the papers of Balk *et al.* [42] and Koyrakh [43].

Aside from these inverse mass power corrections, another technique was developed [22] consisting in a leading twist approximation as familiar from deep inelastic scattering. This new approach stemmed from the observation

that the operator product expansion (OPE), forming the basis of the power corrections, fails at the high endpoint of the electron energy spectrum. This regime turned out to require a separate treatment with new nonperturbative input which was introduced in the form of the so-called shape function. This function describes the light-cone distribution of the b quark within B meson. The light cone approximation holds as long as the final hadrons can be treated as nearly massless. It is worth noting that at this point the effective theory made contact with the phenomenological approach. Indeed, analyses have been done [56] to establish the connexion between the two. At any rate, these essentially model-like descriptions appear to be necessary whenever one focusses on spectra rather than restricting oneself to moments, which are believed to be reproduced correctly from the mass expansion. The shape function does not depend on the final states but rather is inherent to the B meson itself. This in particular means that information gathered from other processes can be used. Along these lines, the case of semileptonic B decays is related [57] to radiative $b \rightarrow s\gamma$ decays. Formally, the leading twist expansion corresponds to resumming the most singular terms in the inverse mass series so that it is perfectly possible to calculate both kinds of corrections and disentangle the different terms in order to avoid double-counting any part. One may think of those two methods as summing the terms appearing in the full result along different paths, and we know which they are.

In the following section we explain our choice of the method of extracting $|V_{ub}|$. Then Sec. 5.3 is devoted to the articulation of both corrections in the desired approximation. Subsequently, we discuss the shape function characterising the nonperturbative input used in our calculations in Sec. 5.4 and then go over to the results in Sec. 5.5.

5.2 Method of measuring V_{ub} .

In our paper, we propose to use the semileptonic B decays in the determination of the V_{ub} element. One of the difficulties to be negotiated is the prevalence of charmed final states, which exceed the charmless ones by a factor of 100. We try to address this problem by imposing an upper cut on the invariant mass of the final hadrons. Since the lowest charmed state has a mass squared of approximately 3.5 GeV^2 , this value suggests the placement of our cut. Whatever the exact value chosen, this kind of cut has consequences on the methods we have to apply. As regards perturbative QCD corrections, we use the one-loop level spectra, which is the best result available. The question is what nonperturbative effects should be included. As mentioned above, there are at least two approaches to the problem. It turns out that the cut on the hadronic mass makes the resulting distributions sensitive to the Fermi motion of the b quark within the decaying meson. Due to this fact, we include the leading twist corrected terms. As explained in the section discussing the HQET expansions, this effectively consists in performing a convolution with the shape function. Thus both the tree level and one-loop terms of the partonic distribution are weighed with this function with the mass of the b quark effectively varied.

The convolution needed to obtain the leading twist approximation requires a choice of the shape function. Since it is of a nonperturbative nature, we need to decide on a model with parameters to be fitted from experimental data. As regards our present knowledge about the shape function, it is usually expressed in terms of its moments and the difference between the meson and quark mass $\bar{\Lambda} = m_B - m_b$. These are not entirely independent quantities, however. The best known moment is the upper limit of the support of the shape function, related to $\bar{\Lambda}$. The first moment vanishes by equation of motion, while the second corresponds to the kinetic energy of the b quark in the meson and is proportional to the parameter λ_1 , which is rather poorly known to date. The third moment is considered in the literature, but we ignore it altogether as little is known about it quantitatively. Summarizing the properties of the shape function $f(m_b^*)$, we can write the following conditions, of which the first is normalisation.

$$\int_{-\infty}^{M_B} f(m_b^*) dm_b^* = 1, \quad (96)$$

$$\int_{-\infty}^{M_B} f(m_b^*)(m_b^* - m_b) dm_b^* = 0, \quad (97)$$

$$\int_{-\infty}^{M_B} f(m_b^*)(m_b^* - m_b)^2 dm_b^* = -\frac{1}{3}\lambda_1, \quad (98)$$

$$\int_{-\infty}^{M_B} f(m_b^*)(m_b^* - m_b)^2 dm_b^* = -\frac{1}{3}\rho_1. \quad (99)$$

In these formulae, m_b^* denotes the effective mass of the b quark. Certainly, as one gets to know the moments of the shape function better, it will be of use to include them all. This is technically reduced to examining the shape function to be used in the convolution for an extended range of parameters.

For our analysis, we have chosen to use the form of the shape function suggested in the BaBar physics book [58], which reads

$$f(m^*) = \tilde{f}\left(\frac{k_+}{\Lambda}\right) \equiv \tilde{f}\left(\frac{m^* - m_b}{\Lambda}\right), \quad (100)$$

with

$$\tilde{f}(x) = N\theta(1-x)e^{c(x-1)}(1-x)^{(c-1)}. \quad (101)$$

We have scanned the results obtained for a couple of parameter sets corresponding to realistic shape functions. The error estimate of 10% which we have arrived at is based upon the range within which the result falls subject to the choice of the nonperturbative and perturbative parameters.

In making our choice of the quantity to be studied, we were also guided by consideration of the mass definition. The quark masses affect the decay widths rather substantially, entering with a fifth power in the overall prefactor. In the prescription of effective mass convolution we have skipped the point of this prefactor. Although it is by no means a proved statement, an analogy to muon capture suggests that these factors, determining the total rate, should

be left constant and that is what we do. Note that this is not the case in the original ACCMM model. Whatever the consequences of the treatment of mass be, however, we hope that we can ease this dependence by considering the ratio of charmless to charmed events.

As already mentioned, our analysis involves a few parameters and two cuts. The most important cut that is freely adjustable is that on the invariant hadronic mass. As will be seen from the results, the greater the cut the weaker the sensitivity to the shape function parameters gets. On the other hand, the very reason for placing this cut, the removal of charmed states, requires it to fall in the vicinity of 3.5 GeV. These two arguments are clearly contradictory and we would not feel comfortable picking one value for all the subsequent analysis. Rather, we have decided to consider this cut as a variable and study the above-mentioned ratio for different values of the cut. It will be seen that too low a cut would mar the result with wild dependence on fine details of the nonperturbative shape function, which we do not know that well. Eventually, the range of 2 GeV² through 4 GeV² will be studied.

5.3 Combining perturbative and nonperturbative corrections

In order to provide means of extracting the ratio of V_{CKM} elements, one has to define a quantity that is to be matched to experimental results. We examine the ratio

$$R = \frac{\Gamma_u(M_{cut}^2, E_{cut})}{\Gamma_c(E_{cut})} \equiv r \frac{|V_{ub}|^2}{|V_{cb}|^2}, \quad (102)$$

where the rates are defined as follows:

$$\Gamma_u(M_{cut}^2, E_{cut}) = \int_0^{M_{cut}^2} dM_X^2 \int_{E_{cut}}^{M_B/2} dE_l \frac{d\Gamma(B \rightarrow X_u e \bar{\nu}_e)}{dM_X^2 dE_l}, \quad (103)$$

$$\Gamma_c(E_{cut}) = \int_{E_{cut}}^{E_{max}} \frac{d\Gamma(B \rightarrow X_c e \bar{\nu}_e)}{dE_l}. \quad (104)$$

In the above formulae, E_{cut} denotes the minimal electron energy, while M_{cut}^2 the maximal hadronic invariant mass squared. For the charmed decay, the maximal electron energy is given by

$$E_{max} = \frac{m_b^2 - m_c^2}{2m_b}, \quad (105)$$

as it is treated in the perturbative approximation to order $\mathcal{O}(\alpha_s)$. Thus the expression for the decay to the charm quark is in fact taken as

$$\Gamma_c(E_{cut}) = \int_{2E_{cut}/m_b}^{1-\rho} \frac{d\Gamma}{dx} dx, \quad (106)$$

which involves partonic distributions only. The mass of the b quark which is taken for this formula is related to the parameter $\bar{\Lambda}$ describing the shape function using the approximation

$$m_b = M_B - \bar{\Lambda}, \quad (107)$$

valid up to $\mathcal{O}(1/m_b^2)$ corrections. Thus the dependence on the shape function actually enters both decay rates defining the ratio (102). The rate of the decay to X_u states is computed taking into account both perturbative corrections to order α_s and the leading twist non-perturbative effects due to the Fermi motion, which are expressed in terms of the shape function $f(m^*)$. The resulting distribution is

$$\begin{aligned} \frac{d\Gamma}{dM_X^2 dE_l} = & \int_0^1 dx \int_{1-x}^{2-x} dx_p \int_{z_{min}}^{z_{max}} dz \int_{-\infty}^{M_B} dm^* f(m^*) \frac{d\Gamma^{parton}}{dxdx_pdz} \times \\ & \delta(M_X^2 - m^{*2}z - x_p \bar{\Lambda}^* m^* - \bar{\Lambda}^{*2}) \delta(E_l - \frac{m^* x}{2}). \end{aligned} \quad (108)$$

The partonic rate can be split into the tree level term and the $\mathcal{O}(\alpha_s)$ correction,

$$d\Gamma^{parton} = d\Gamma^{parton,0} + \frac{2\alpha_s}{3\pi} d\Gamma^{parton,1}, \quad (109)$$

and then the convoluted rate can be divided up accordingly. Using the delta functions, the integrations involved in these rates can be simplified, yielding,

$$\begin{aligned} & \int_{E_{cut}}^{M_B/2} dE_l \int_0^{M_{cut}^2} dM_X^2 \frac{d\Gamma^{(0)}(B \rightarrow X_u e \bar{\nu}_e)}{dM_X^2 dE_l} = \\ & \int_{E_{cut}}^{M_B/2} dE_l \int_{2E_l/M_B}^1 dx \int_{y_{min}}^x dy \frac{2}{x} f\left(\frac{2E_l}{x}\right) \frac{d\Gamma^{parton,0}}{dxdy}, \end{aligned} \quad (110)$$

$$y_{min} = \max\{0, \frac{1 - M_{cut}^2 - (M_B - 2E_l/x)^2}{(2E_l/x)(M_B - 2E_l/x)}\} \quad (111)$$

for the tree level contribution, while the α_s correction contributes

$$\begin{aligned} & \int_{E_{cut}}^{M_B/2} dE_l \int_0^{M_{cut}^2} dM_X^2 \frac{d\Gamma^{(1)}(B \rightarrow X_u e \bar{\nu}_e)}{dM_X^2 dE_l} = \\ & \int_{E_{cut}}^{M_B/2} dE_l \int_{2E_l/M_B}^1 dx \int_{1-x}^{2-x} dx_p \int_{z_{min}}^{z_{max}} dz \frac{2}{x} f\left(\frac{2E_l}{x}\right) \frac{d\Gamma^{parton,1}}{dxdx_pdz} \end{aligned} \quad (112)$$

where

$$z_{min} = \begin{cases} 0, & \text{for } x_p \leq 1, \\ x_p - 1 & \text{for } x_p > 1, \end{cases} \quad (113)$$

and

$$z_{max} = \min\left\{\frac{M_{cut}^2 - x_p(M_B - 2E_l/x) - (M_B - 2E_l/x)^2}{(2E_l/x)^2}, (1-x)(x_p + x - 1)\right\}. \quad (114)$$

The integral over z in Eq. (112) has been performed analytically so that we use the prime function $F(x, x_p, z)$ defined as

$$F(x, x_p, z) = \int_{z_{min}}^z dz' \frac{d\Gamma^{parton,1}}{\Gamma_0 dx dx_p dz'}. \quad (115)$$

$$F = \begin{cases} F_1(z) - F_1(0) + F_2(z) + F_3, & x_p < 1, \\ F_1(z) - F_1(z_{min}) + F_2(z) - F_2(z_{min}) & x_p > 1, \end{cases} \quad (116)$$

where

$$z_{min} = x_p - 1, \quad (117)$$

and

$$\begin{aligned} F_1 = & \frac{1}{8} \left[\frac{1}{t} \ln \frac{1+t}{1-t} [x_p^2 - 4(x-1+x_p/2)^2/t^2] + 8(x-1+x_p/2)^2/t^2 \right] \\ & \times (36 - 39x_p + 12x_p^2 - 3x_p^3/4) + \frac{1}{t} \ln \frac{1+t}{1-t} (x-1+x_p/2)[48 - 78x_p \\ & + 45x_p^2 - 21x_p^3/2 + 3x_p^4/4 + (x-1+x_p/2)(-42 - 15x_p + 27x_p^2 \\ & - 21/8x_p^3)] + (A_1 t + A_2) \ln \frac{1+t}{1-t} + A_3 \log(1-t) + A_4. \end{aligned} \quad (118)$$

$$F_2 = 12[2 \ln^2 z - (8 \ln x_p - 7) \ln z]v(\bar{x} - x_p), \quad (119)$$

$$\begin{aligned} F_3 = & (x_p - \bar{x}) \{ 24 \ln x_p (-1 + 5v - 4v \ln x_p) \\ & + v[-16\pi^2 - 60 - 48 \text{Li}_2(1 - x_p)] \}. \end{aligned} \quad (120)$$

In the above formulae,

$$\begin{aligned} A_1 = & (x_p - \bar{x})(x_p z \bar{x}/2 + 21x_p \bar{x}/2 - 6x_p v - 12x_p^2 \bar{x} + 3x_p^2 v + 7x_p^3 \bar{x}/4) \\ & + (2x_p z v - 9x_p z/2 - 9/10x_p z^2 - x_p^2 z v + 7x_p^2 z + 12x_p^2 v + 15x_p^2/2 \\ & - 21x_p^3 z/20 + 17x_p^3 v/2 - 105/4x_p^3 - 5/4x_p^4 v + 53/4x_p^4 \\ & - 219/160x_p^5), \end{aligned} \quad (121)$$

$$\begin{aligned} A_2 = & (x_p - \bar{x})(-36x_p(1 - x_p x) + 6x_p^2 v + 4x_p^3 \bar{x} + 12\bar{x} - 96v \ln 2 + 48v) \\ & - 24x_p + 48x_p^2 + 16x_p^3 v - 60x_p^3 - 2x_p^4 v + 26x_p^4 - 12/5x_p^5, \end{aligned} \quad (122)$$

$$A_3 = 2A_2 + 96(x_p - \bar{x})(1 + \bar{x} - x_p) \ln(1 + t), \quad (123)$$

$$\begin{aligned} A_4 = & (x_p - \bar{x})(5x_p z \bar{x} - 24z \bar{x} + 12z v) + 32x_p z v - 81x_p z - 21/5x_p z^2 \\ & - 4x_p^2 z v + 40x_p^2 z - 81/20x_p^3 z + 36z v + 12z - 6z^2 v + 24z^2, \end{aligned} \quad (124)$$

and

$$\bar{x} = 1 - x, \quad v = 2 - x - x_p, \quad t = \sqrt{1 - 4z/x_p^2}. \quad (125)$$

5.4 Shape function parameters

The decay rate distributions depend on the strong coupling constant, α_s , as well as the parameters characterizing the shape function. The latter are identified

with the meson-quark mass difference $\bar{\Lambda}$ and the quark kinetic energy inside the meson, $-\frac{1}{3}\lambda_1$. These physical quantities make their appearance in the shape function according to the BaBar ansatz [58],

$$f(m^*) = \tilde{f}\left(\frac{k_+}{\bar{\Lambda}}\right) \equiv \tilde{f}\left(\frac{m^* - m_b}{\bar{\Lambda}}\right), \quad (126)$$

with

$$\tilde{f}(x) = N\theta(1-x)e^{c(x-1)}(1-x)^{(c-1)}. \quad (127)$$

The normalizing factor N is given by

$$N = \frac{c^c}{\Gamma(c)\bar{\Lambda}}, \quad (128)$$

and the parameter c is related to the physical ones by

$$c = \frac{-3\bar{\Lambda}^2}{\lambda_1}. \quad (129)$$

We have considered a set of parameters $\bar{\Lambda}, \lambda_1$. They are believed to fall in the ranges

$$0.3 \text{ GeV} \leq \bar{\Lambda} \leq 0.5 \text{ GeV}, \quad -0.6 \text{ GeV}^2 \leq \lambda_1 \leq -0.1 \text{ GeV}^2. \quad (130)$$

However, we have also imposed the condition that the mean kinetic energy of the quark should not exceed considerably the meson-quark mass difference. For α_s we have used

$$\alpha_s \in \{0.2, 0.3\}, \quad (131)$$

For each value of α_s , the following sets of non-perturbative parameters have been examined:

$$\bar{\Lambda} = 0.3 \text{ GeV}, \quad \lambda_1 = -0.1 \text{ GeV}^2, \quad (132)$$

$$\bar{\Lambda} = 0.3 \text{ GeV}, \quad \lambda_1 = -0.2 \text{ GeV}^2, \quad (133)$$

$$\bar{\Lambda} = 0.3 \text{ GeV}, \quad \lambda_1 = -0.25 \text{ GeV}^2, \quad (134)$$

$$\bar{\Lambda} = 0.5 \text{ GeV}, \quad \lambda_1 = -0.1 \text{ GeV}^2, \quad (135)$$

$$\bar{\Lambda} = 0.5 \text{ GeV}, \quad \lambda_1 = -0.4 \text{ GeV}^2, \quad (136)$$

$$\bar{\Lambda} = 0.5 \text{ GeV}, \quad \lambda_1 = -0.6 \text{ GeV}^2. \quad (137)$$

The parameters of the shape function as well as the value of the coupling constant have a twofold effect on the examined ratio r since both the numerator and the denominator of the expression depend on those numbers. The decay rate to charmless states has the dependence encoded in the convolution with the shape function and the perturbative corrections. The charmed rate depends on the $\bar{\Lambda}$ parameter through the ratio of b to c quark masses. The Born rate normalised to Γ_0 of $b \rightarrow c$ decay is

$$\Gamma = 0.44064 \quad \text{for } \bar{\Lambda} = 0.3 \text{ GeV},, \quad (138)$$

$$\Gamma = 0.49938 \quad \text{for } \bar{\Lambda} = 0.5 \text{ GeV}, \quad (139)$$

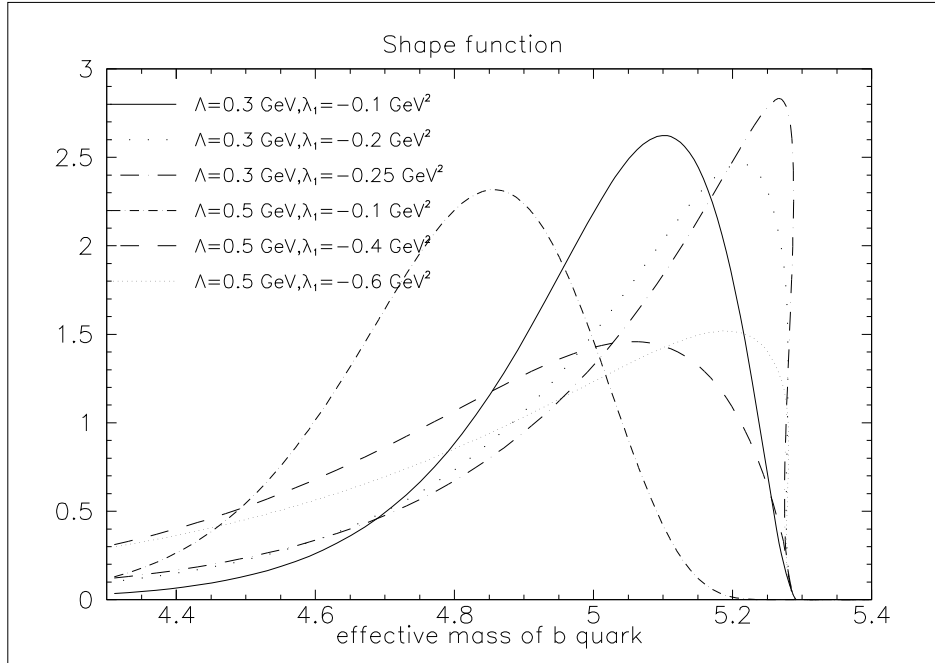


Figure 2: Shape function $f(m^*)$ for different values of $\bar{\Lambda}$ and λ_1 .

where the electron energy cut was set to $E_{cut} = 0.5$ GeV.

The shape function corresponding to the 6 sets of parameters is plotted as a function of the effective b quark mass in Fig.2. For clearer distinction see Figs. 3 and 4.

5.5 Results

5.5.1 General result on $|V_{ub}|$ accuracy.

If we choose $M_X^2 = 4$ GeV 2 as the hadronic mass squared cut, then the uncertainty of the extracted value of $|V_{ub}|$ will be about 10%. The source of this uncertainty lies with the parameters that go into it. The quantity r which we have chosen for use in the determination of the ratio of $|V_{ub}/V_{cb}|$ depends on the strong coupling constant, the quark masses and the parameters $\bar{\Lambda}$ and λ_1 entering the shape function. This makes for quite an involved structure of the various contributions. Before we specify and discuss these, let us briefly recall the range of the survey that has been performed. In order to make a prediction, we have examined the various sets of parameters as defined by Eq.(132-137). The six sets of nonperturbative parameters span a conservative range of the estimates for the meson-quark mass difference ($\bar{\Lambda}$) and the kinetic energy of the b quark Fermi motion (λ_1). In addition, the strong coupling constant was taken to be 0.2 or 0.3 for each set, while the electron energy cut was kept constant

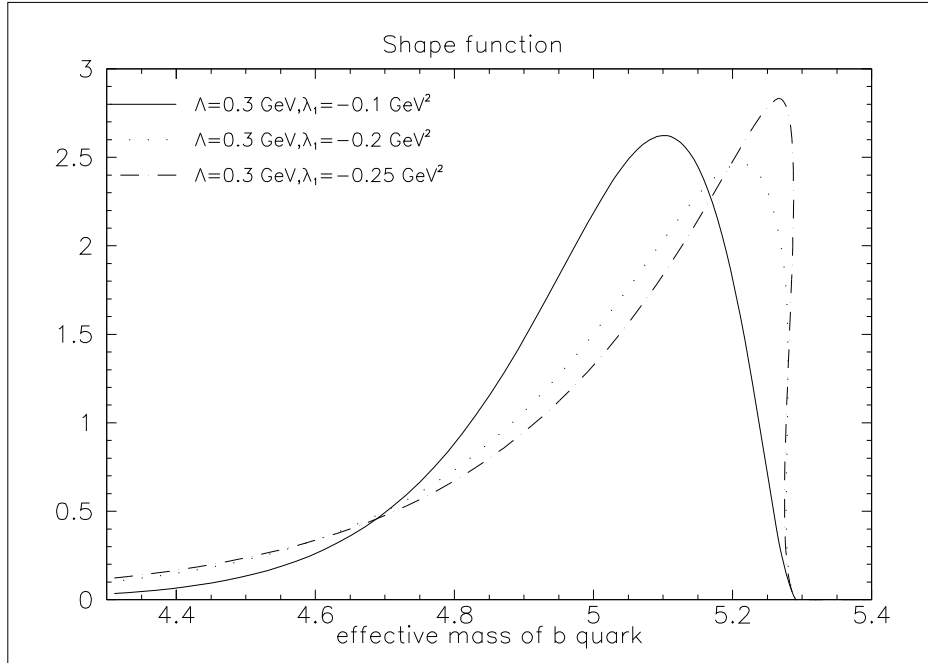


Figure 3: Shape function for $\bar{\Lambda} = 0.3$ GeV.

at all times and set to 0.5 GeV. This particular cut is arguably of minor importance to the analysis and has been made to provide for the identification of the semileptonic mode. More vital is the remaining upper cut on the hadronic invariant mass. We look closer at the range of 2 GeV^2 to 4 GeV^2 of this cut.

By examining the variation of the observable r due to the changes of the parameters we can obtain an estimate of the accuracy that can be achieved. The form of the function $r(M_X^2)$ obtained for all the studied sets has been presented in Fig. 11. The value of $r(M_{cut}^2 = 4 \text{ GeV})$ can be approximately written as

$$r = 1.74 + 0.3 \frac{\Delta \alpha_s}{\tilde{\alpha}_s} + 0.2 \frac{\Delta \bar{\Lambda}}{\bar{\Lambda}} + 0.08 \frac{\Delta \lambda_1}{\lambda_1}. \quad (140)$$

These numbers give a flavour of the dependence on the parameters. Let us now turn to the identification of the effects brought about by the nonperturbative and perturbative corrections. Since it is the hadronic invariant mass cut that is variable in our analysis, we will look at the value of the examined ratio r as a function of this cut, $r(M_X^2)$. We will look at the partonic result at the Born level and at the corrections it receives from the perturbation theory as well as HQET leading twist approximation.

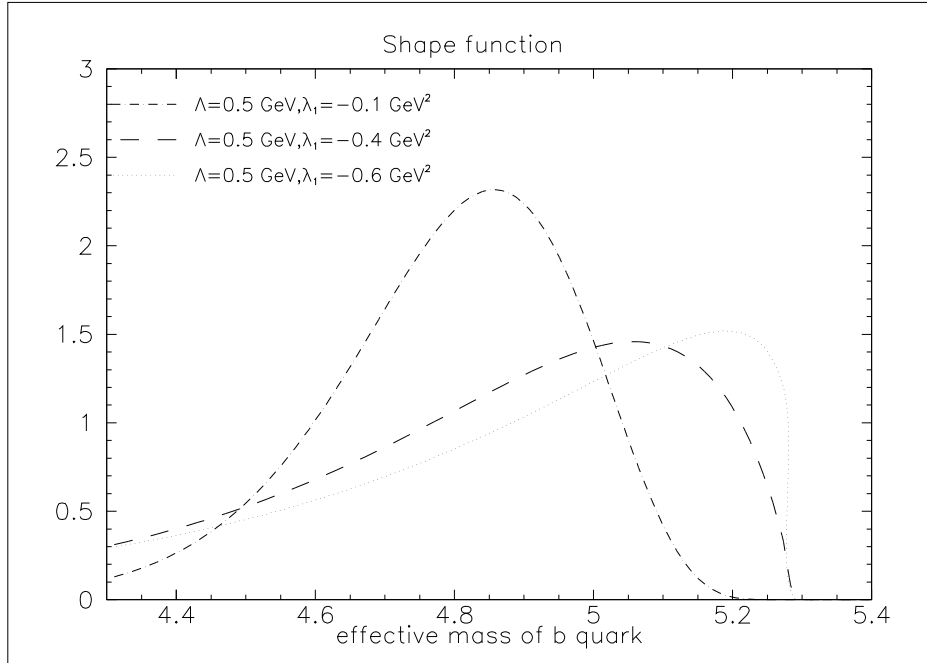


Figure 4: Shape function for $\bar{\Lambda} = 0.5$ GeV.

5.5.2 Partonic results.

Although it might appear that partonic results, understood to treat the decay as that of a free quark into a free quark and a pair of free leptons, have little in common with nonperturbative data, the latter intrude via the quark mass ratio. This is a simple consequence of the difficulty that arises as soon as one tries to treat quarks as free, ignoring confinement. Thus, while the $b \rightarrow u$ decay rate is truly devoid of any reference to nonperturbative quantities in this zeroth approximation, the decay to charmed states will bear a mark of the $\bar{\Lambda}$ parameter, which sets the b quark mass. The values of the scaled decay rates have been quoted in Eqs.(138,139). With the mass of the b quark fixed, the ratio can also be thought of as fixed due to the fairly well known mass difference between b and c quarks of 3.4 GeV. Curiously enough, we must conclude that if we only considered the partonic result, the fact that we are calculating ratio rather than the rate itself would be counterproductive to precision. But of course such reasoning would be unrealistic as the corrections are essential to accuracy and must be included. We do not present any plots for the partonic quantity of $r(M_X^2)$. Since the invariant mass of the hadrons is always zero in this approach, such plots would have to be series of horizontal lines. However, beneath we give the parton model values of r obtained assuming $\bar{\Lambda} = 0.3$ GeV and $\bar{\Lambda} = 0.5$ GeV.

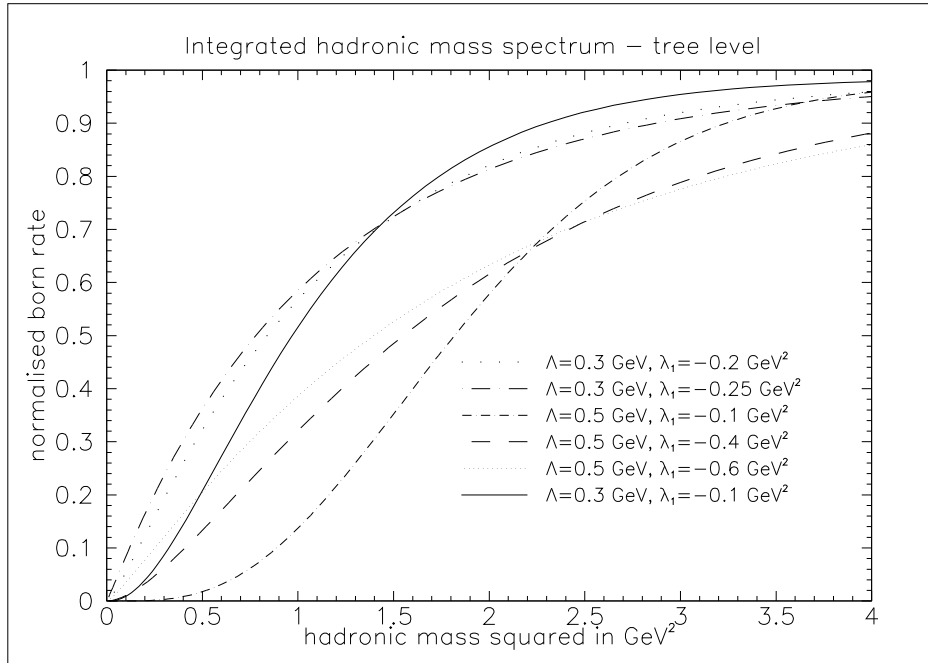


Figure 5: $B \rightarrow X_u$ decay rate at tree level.

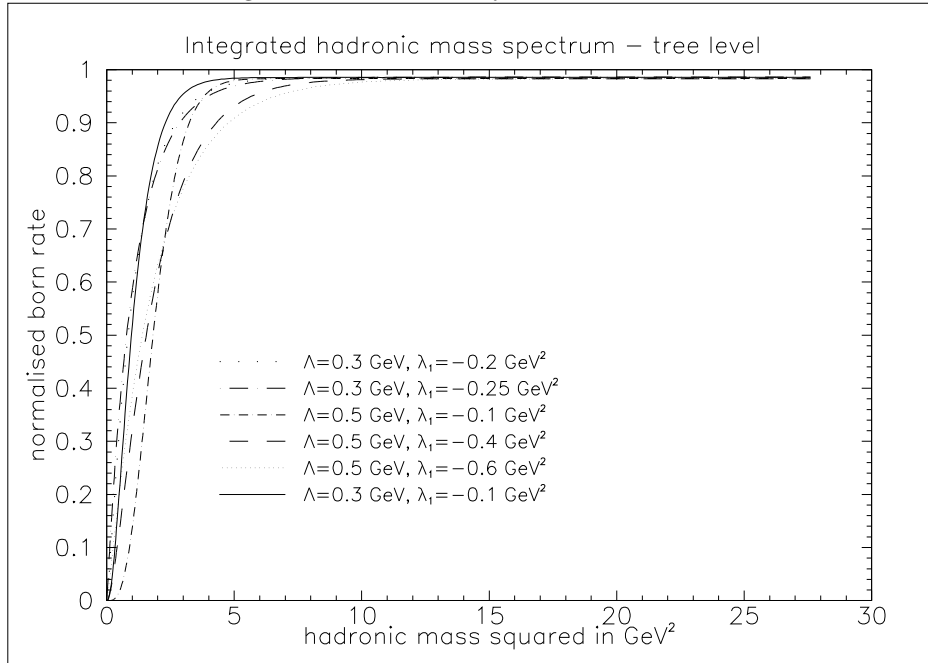


Figure 6: $B \rightarrow X_u$ decay rate at tree level in the whole range of hadronic mass.

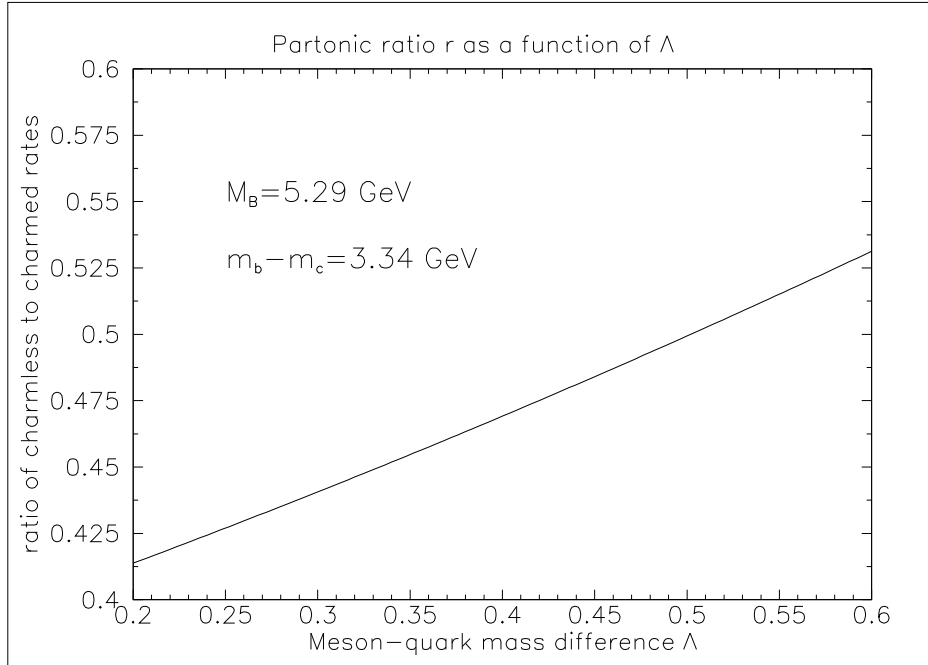


Figure 7: The partonic value of the ratio r of charmless and charmed decays as dependent on the $\bar{\Lambda}$ parameter.

They are clearly the reciprocals of the scaled rates stated in Eqs.(138,139).

$$r = 2.2694 \text{ for } \bar{\Lambda} = 0.3 \text{ GeV}, \quad (141)$$

$$r = 2.0025 \text{ for } \bar{\Lambda} = 0.5 \text{ GeV}. \quad (142)$$

The dependence of the partonic value of r on the parameter $\bar{\Lambda}$ is nearly linear in any reasonable interval, as seen in Fig. 7.

5.5.3 Convolved partonic results.

The rather dull hadronic mass spectrum delivered by the partonic model gains colour when the Fermi motion is accounted for. The distribution gets indented at the lower end of the spectrum because now the hadronic mass is taken to incorporate also the 'brown muck' or the light degrees of freedom, or, couched in the language of phenomenological models, the spectator. This kinematical argument is relevant even though we are dealing with a formally developped approximation to QCD, which renounces model dependence. This is because the kinematics of this approximation is clear. The b quark is static with its mass, as it were, bulging or shrinking. The conservation of four-momentum then leads to a unique expression for the hadronic invariant mass,

$$M_X^2 = m^{*2}z - x_p \bar{\Lambda}^* m_b^* - \bar{\Lambda}^{*2}. \quad (143)$$

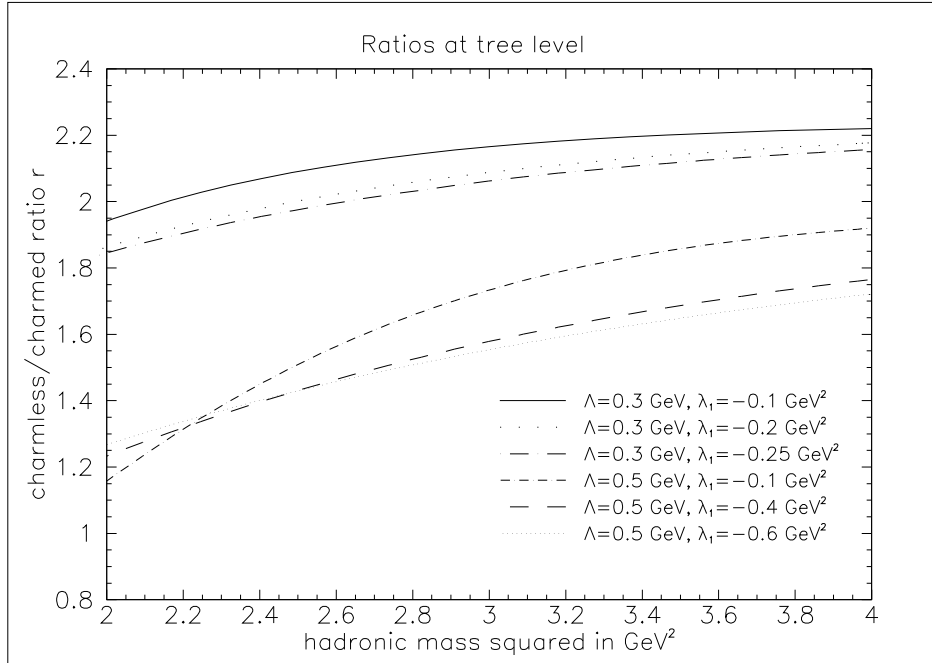


Figure 8: Ratios charmless/charmed at tree level.

This formula implies that the typical scale on which the effects of including the Fermi motion are expected to be noticeable is set by $\bar{\Lambda}m_b$, which is around 2 GeV and whose variations are discernible. The extent to which the light constituents of the B meson exert influence over the hadronic mass distribution is gauged by the parameters of the shape function. In particular, the departure of the b quark mass from the mass of the meson, as indicated by $\bar{\Lambda}$, shows positive correlation with the shift of the distribution, see Fig. 5 showing the rates and Fig. 8 for the ratio $r(M_X^2)$. Note that the probabilistic nature of the convolution implies that barring the effects of the imposed cuts one should recover the partonic results upon phase space integration. That this does happen is visible from Fig. 6 where the different sets tend to a common value as the hadronic mass is cut sufficiently high.

5.5.4 Convolved one-loop corrections.

As explained in Sec. 5.3, the perturbative corrections are combined with the nonperturbative ones in essentially the same way as the tree level partonic term. It is well known that one-loop corrections themselves yield a singular hadronic mass distribution, characterised by a Dirac delta peak at zero mass and a continuous but divergent part. The Kinoshita-Lee-Nauenberg theorem [10, 11], ensures that the divergences cancel once they are properly regularised. In a

strict perturbation theory, final results are only obtained upon integration over some final range of the invariant mass, enclosing an interval around zero. The convolution prescribed in the leading twist approximation performs this integration so that no infinity enters the one-loop corrected and convoluted terms, as seen in Fig. 9. However, the large negative correction remains in the convoluted spectra as a dip close to the lower end. As with the tree level result, the corrections are affected by the Fermi motion in a degree that depends on the size of the applied hadronic mass cut. Clearly, the low end of the spectrum is very sensitive to the details of the shape function, while this influence is washed out above the rough scale of $\bar{\Lambda}m_b$. Again, we recover the partonic result after inclusion of all phase space, see Fig. 10.

5.5.5 Perturbative and nonperturbative corrections.

Summarizing, it is seen that although low cuts on the hadronic mass are favoured by the requirement of cutting off the charmed admixture, they leave the resulting distribution uncomfortably dependent on the Fermi motion. This motion is known via the moments of the shape function and since this knowledge is not very accurate we cannot rely on the details of it. Therefore we suggest that to be conclusive one must take the cut at least at the level of $M_X^2 = 2$ GeV. On the other hand, to prevent the charmed states from excessive proliferation and swamping the charmless events, we do not consider values higher than $M_X^2 = 4$ GeV.

Deciding upon these ranges, we can come to conclusions about the attainable accuracy of $|V_{ub}|$ as measured in the way we propose. To this end, we have collected the calculated values of the ratio $r(M_X^2)$ in Fig. 11. The spread of the ratio for a given cut reflects the uncertainty ascribed to the measurement of the square of the matrix element. Thus, if one sets the cut to 4 GeV, one can hope of extracting $|V_{ub}|$ with an uncertainty of around 10%.

5.5.6 Discussion of uncertainty.

The above conclusion regarding the precision we assign to our method aims to be conservative and it is based on a scan of a wide range of parameters entering the distributions. However, it is possible to improve on the accuracy of these parameters. It might be useful to exploit the analogy to the $b \rightarrow s\gamma$ decays and extract the nonperturbative information from them, as suggested in [57]. On the other hand, the question remains whether one can use other observables of the semileptonic decays to help establish parameters. This latter method has the advantage of eliminating possible systematic errors due to different kinds of considered processes.

We have taken a look at the differential distribution of the hadronic mass. This is to be distinguished from the integrated distribution discussed so far. As already seen, this quantity is sensitive to the details of the shape function. One can see this for oneself in Fig. 16 for $\bar{\Lambda} = 0.3$ GeV and Fig. 17 for $\bar{\Lambda} = 0.5$ GeV. The contribution from the tree level term is presented in Figs. 12 and 13

for a broader range of the hadronic mass. Similarly, the one-loop corrections themselves have been shown in Figs. 14, 15.

5.6 Summary

We calculate corrections of perturbative and nonperturbative nature to the hadronic mass spectrum in the semileptonic B decays. One-loop results are convoluted with the shape functions to give predictions of the $|V_{ub}|$ matrix element with an uncertainty of 10%. This error estimate relies on the current knowledge of parameters characterising the B mesons. We state the functional dependence of the errors in terms of the involved parameters so that an estimate can be made in case the precision of the latter is improved on. We also suggest an observable to be employed in determining these parameters from the semileptonic decays and present the prediction for it through one-loop level supplemented by leading twist corrections.

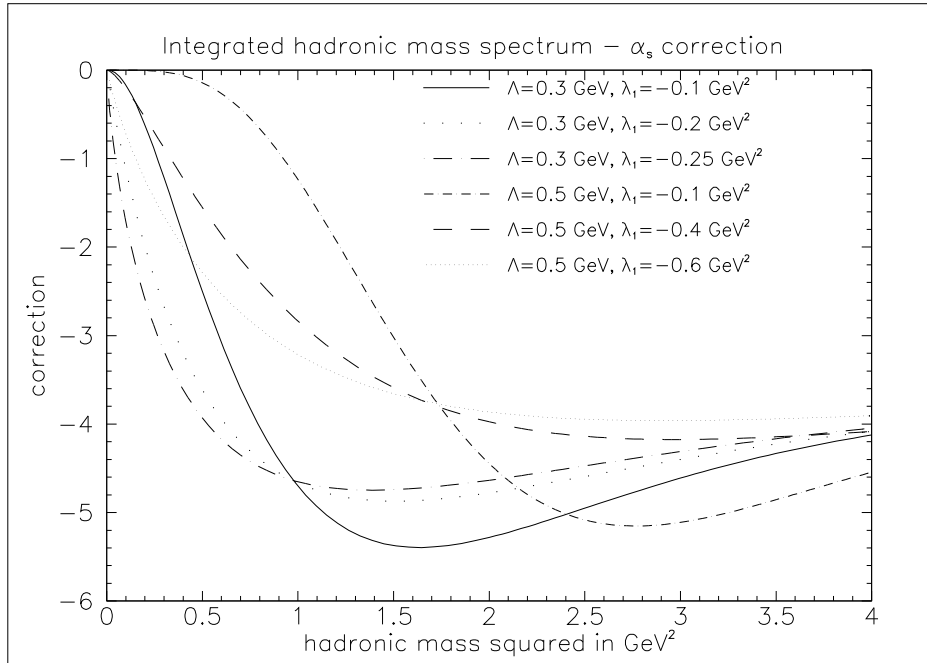


Figure 9: Perturbative correction to integrated hadronic mass spectrum.

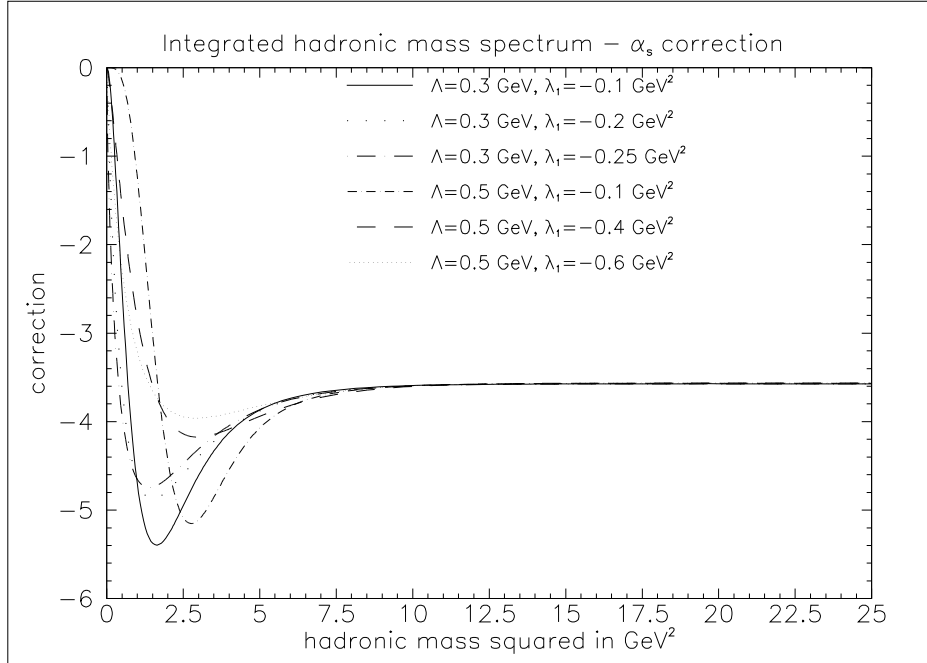


Figure 10: Perturbative correction to integrated hadronic mass spectrum.

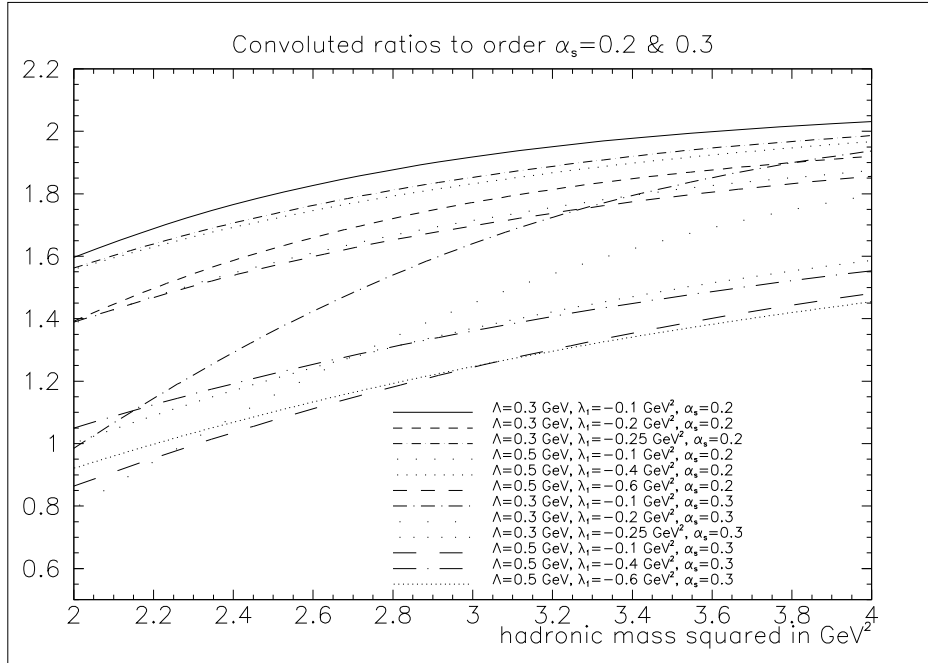


Figure 11: Ratios r for all the examined sets of parameters.

6 Longitudinal polarisation of τ lepton

6.1 Introduction

The longitudinal polarisation of the τ lepton is a non-trivial quantity due to the large mass of the tauon. This is contrary to the electron or even muon, whose masses are so small that the $V - A$ structure of the interaction causes them to be practically completely left-handed upon production in B decays. The polarisation itself is an interesting quantity as it can provide means of measuring the quark masses, especially the difference between b and c quark masses. Unlike the rate itself, the polarisation is regular throughout the range of the charged lepton energy even after inclusion of one-loop corrections. Furthermore, the dependence on the poorly known CKM matrix elements is eliminated. The need for calculating the correction to this quantity is apparent given that the decay rate receives as much as 20% contribution from the one-loop diagrams. It is therefore all the more remarkable that the situation is in the end different for the polarisation. It turns out, as the calculation below shows, that the polarisation receives only a tiny correction. In view of the poor knowledge of the strong coupling constant, this kind of cancellation is also interesting when one considers extracting quark masses from this quantity. The first indication of the smallness of the radiative correction to the τ longitudinal polarisation

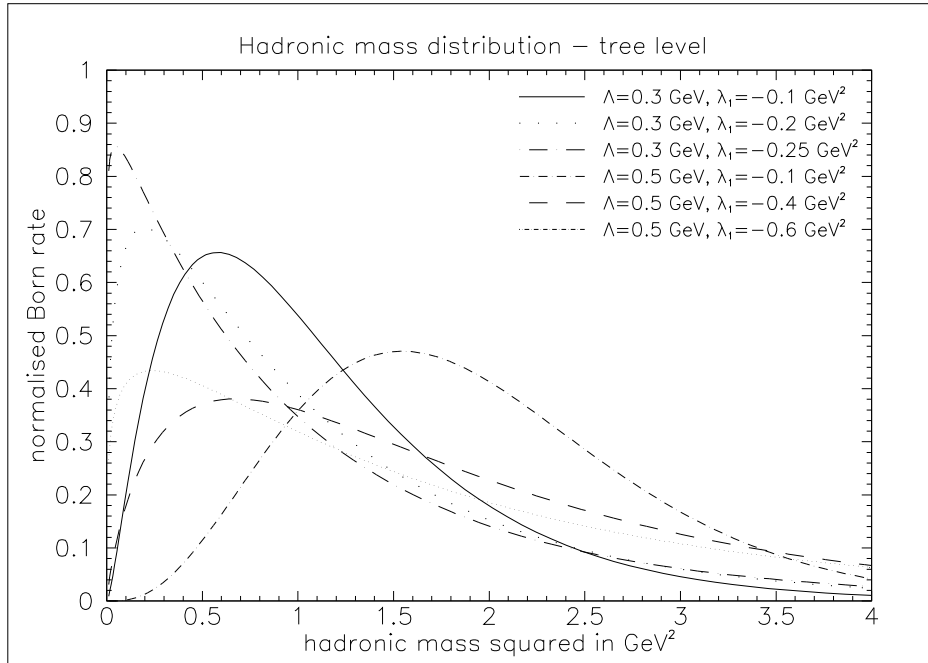


Figure 12: Hadronic mass distributions at tree level.

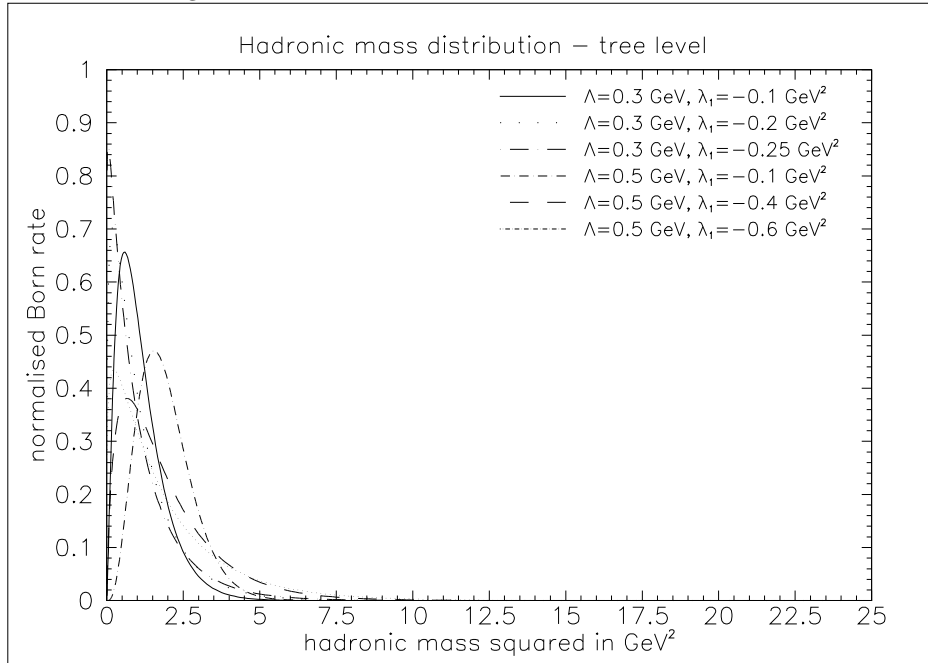


Figure 13: Hadronic mass distributions at tree level.

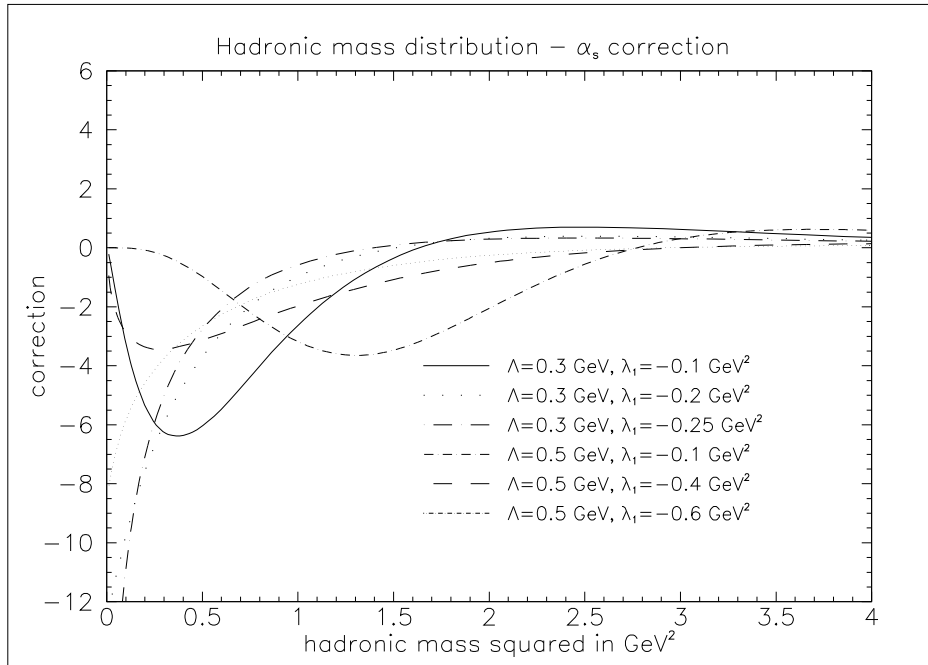


Figure 14: $\mathcal{O}(\alpha_s)$ correction to hadronic mass distribution.

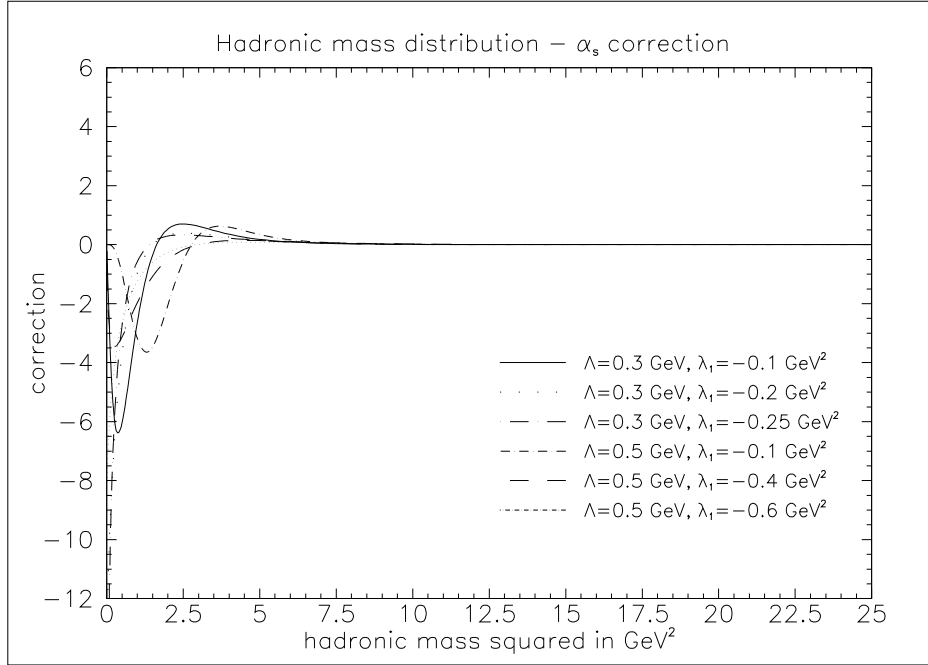


Figure 15: $\mathcal{O}(\alpha_s)$ correction to hadronic mass distribution.

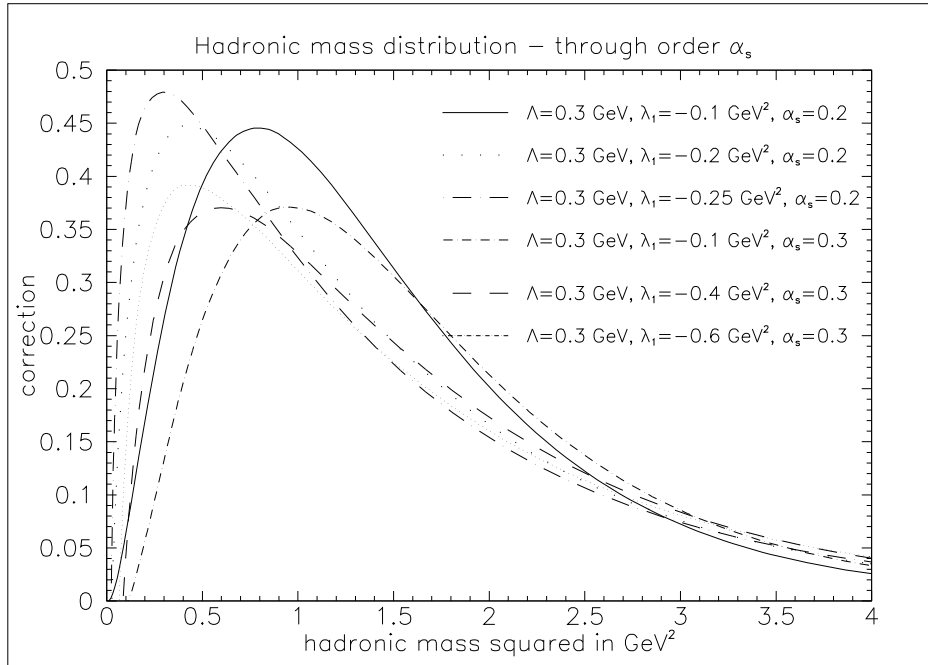


Figure 16: Hadronic mass distributions to order α_s for $\bar{\Lambda} = 0.3$ GeV.

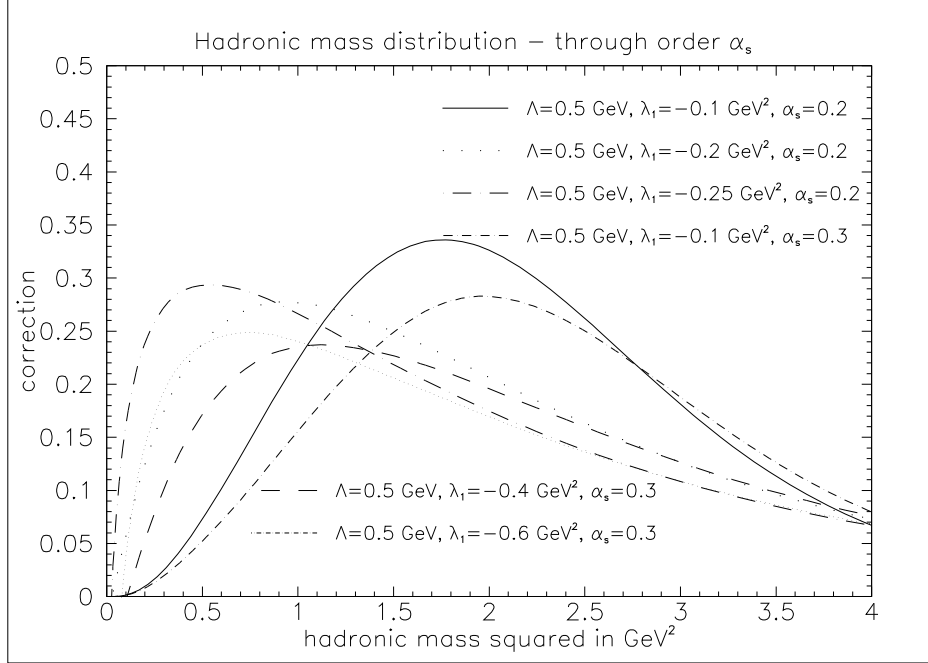


Figure 17: Hadronic mass distributions to order α_s for $\bar{\Lambda} = 0.5$ GeV.

was found in [35] where this quantity was calculated in the rest frame of the pair of leptons.

In order to find the polarisation, one may proceed as follows. First we get the result for the unpolarized distribution, as found in [36, 37]. Then we are left with the task of finding the decay rate into either state of polarisation of the charged lepton. It seems natural, taking into account the structure of the weak interactions, that we calculate the rate of decay into a negatively polarized electron. Thus we present formulae for the double distribution in terms of the lepton energy and the invariant mass of the intermediate W boson. Combining these with the formulae for the unpolarized rate we readily find the polarisation. We also integrate the rate over the invariant mass of W to obtain the charged lepton energy spectrum. This allows us to evaluate the polarisation in terms of the tauon energy, which is shown in a plot.

When giving the results for the polarisation we also use the nonperturbative corrections of order $1/m_b^2$, found in [45] for the polarised lepton. That paper also gives the unpolarised distributions in the mass expansion, which were first calculated in [42] and [43]. The HQET corrections appear in the form of extra terms proportional to the phenomenological constants λ_1 and λ_2 . While the second of them can be related to the mass splitting between vector and pseudoscalar B mesons due to chromomagnetic interaction, and is therefore fairly well established, the parameter λ_1 refers to the kinetic energy of the Fermi motion of the b quark within the meson and only rough estimates can be made of it. It is thus convenient to express any corrections in terms of factors multiplying these parameters, which we do. This part of the paper starts with a description of the evaluation of the polarisation in Sec. 6.2, which is followed by the results given in an analytical form in Sec. 6.3. The method of incorporating the QCD corrections has been discussed in Sec. 3.1. Later on the moments of lepton energy distribution are studied, Sec. 6.4, and we summarize the results.

6.2 Evaluation

Let us start with the tree level matrix element for the unpolarized decay rate:

$$\mathcal{M}_{0,3}^{un}(\tau) = q \cdot \tau Q \cdot \nu. \quad (144)$$

With this kind of linear dependence on the four-momentum τ , it is worth noting that the matrix element with the τ polarisation taken into account is,

$$\mathcal{M}_{0,3}^{pol} = \frac{1}{2} \mathcal{M}_{0,3}^{un}(K = \tau - ms) = \frac{1}{2} (q \cdot K)(Q \cdot \nu), \quad (145)$$

where m stands for the lepton's mass and we have introduced the four-vector K

$$K = \tau - ms. \quad (146)$$

This relation is rendered useful by expressing the polarisation four-vector s in the following way:

$$s = \mathcal{A}\tau + \mathcal{B}Q \quad (147)$$

This is correct due to the fact that now only the temporal component of Q does not vanish, whereas the spatial parts of s and τ are parallel. The coefficients \mathcal{A}, \mathcal{B} appearing in the formula above can be evaluated using the conditions defining the polarisation four-vector s :

$$s^2 = -1 \quad (148)$$

$$s \cdot \tau = 0. \quad (149)$$

Upon this one arrives at the following expressions:

$$\mathcal{A}^\pm = \pm \frac{1}{\sqrt{\eta}} \frac{x}{\tau_+ - \tau_-}, \quad (150)$$

$$\mathcal{B}^\pm = \mp \frac{2\sqrt{\eta}}{\tau_+ - \tau_-}. \quad (151)$$

where the superscripts at \mathcal{A}, \mathcal{B} denote the polarisation of the lepton.

Applying now the representation (147) of the polarisation s we readily obtain the following useful formula for the matrix element with the lepton polarized:

$$\mathcal{M}_{0,3}^\pm = \mp \frac{\tau_\mp}{\tau_+ - \tau_-} \mathcal{M}_{0,3}^{un}(\tau) \pm \frac{\eta}{\tau_+ - \tau_-} \mathcal{M}_{0,3}^{un}(Q). \quad (152)$$

The first term on the right hand side of (152) can be calculated immediately once we know the result for the unpolarized case. Thus the problem reduces to performing this calculation again with the only difference amounting to replacing the four-momentum τ of the lepton with that of the decaying quark, Q . The Born-approximated τ energy distribution can be written explicitly as

$$\frac{d\Gamma^\pm}{dx} = 12\Gamma_0 f_0^\pm(x), \quad (153)$$

where

$$\Gamma_0 = \frac{G_F^2 m_b^5}{192\pi^3} |V_{CKM}|^2. \quad (154)$$

The Born level function $f_0(x)$ reads, for the unpolarized case,

$$f_0(x) = \frac{1}{6} \zeta^2 \tau_3 \{ \zeta [x^2 - 3x(1 + \eta) + 8\eta] + (3x - 6\eta)(2 - x) \}, \quad (155)$$

while the polarized cases are obtained using the function Δf_0 :

$$\Delta f_0(x) = \frac{1}{12} \tau_3^2 \zeta^2 \{ \zeta (3 - x - \eta) + 3(x - 2) \}, \quad (156)$$

in the following way:

$$f_0^\pm(x) = \frac{1}{2} f_0(x) \pm \Delta f_0(x). \quad (157)$$

In the formulae above,

$$\tau_3 = \sqrt{x^2 - 4\eta}, \quad \zeta = 1 - \frac{\rho}{1 - x + \eta}. \quad (158)$$

At the tree level, one can express the polarisation integrated over the energy of the charged lepton as well:

$$\begin{aligned}
P = & 1 - 1/18 \left\{ -24\eta^2 + (x_m^3 - 8\eta^{3/2})(3 + \eta - 3\rho) + \right. \\
& 12\eta(x_m^2) - 3x_m^4/2 + 3(1 - \eta)^3(\rho - \rho^3/s^4) + \\
& 3(-1 + \eta)\rho(1 - \rho/s^2)[3(1 - \eta)^2 + \rho(3 + 5\eta)] + 3T_3S/2 + \\
& 3(x_m - 2\sqrt{\eta})(-12\eta - 4\eta^2 + 12\eta\rho - 3\rho^2 + 3\eta\rho^2 + \rho^3) - \\
& 12\eta\rho^3 \ln(s^2/\rho) - 18(2\eta^2 - \rho^2 - \eta^2\rho^2) \ln[2\sqrt{\eta}/(x_m + T_3)] + \\
& 18(1 - \eta^2)\rho^2 \ln(2s^2\sqrt{\eta}/[(1 - \eta)(1 - \eta - T_3) - \rho - \eta\rho]) \} \\
& / \{ T_3S/12 + (2\eta^2 - \rho^2 - \eta^2\rho^2) \ln[(x_m + T_3)/(2\sqrt{\eta})] \\
& \left. - (1 - \eta^2)\rho^2 \ln\{2\sqrt{\eta}\rho/[(1 - \eta)(1 - \eta + T_3) - \rho - \eta\rho]\} \right\}, \quad (159)
\end{aligned}$$

where

$$s = 1 - \sqrt{\eta}, \quad T_3 = \sqrt{x_m^2 - 4\eta}, \quad (160)$$

$$S = 1 - 7[(1 + \eta)(\eta + \rho^2) + \rho(1 + \eta^2)] + \eta^3 + \rho^3 + 12\eta\rho. \quad (161)$$

Noting that the decomposition of the polarisation four-vector affects the leptonic tensor only, one sees immediately that it can also be applied to the QCD corrections.

6.3 Analytical results

The following formula gives the differential rate of the decay $b \rightarrow \tau\bar{\nu}X$, X standing for a c quark or a pair of c and a gluon, once the lepton is taken to be negatively polarized:

$$\frac{d\Gamma^-}{dx dt} = \begin{cases} 12\Gamma_0 \left[F_0^-(x, t) - \frac{2\alpha_s}{3\pi} F_{1,A}^-(x, t) \right] & \text{for } (x, t) \text{ in A} \\ 12\Gamma_0 \frac{2\alpha_s}{3\pi} F_{1,B}^-(x, t) & \text{for } (x, t) \text{ in B} \end{cases} \quad (162)$$

F_1^- differs according to which region (A or B) it belongs to. Region A is available for the 3- and 4-body decay, while Region B with a gluon only. The following formulae are given for the negative polarisation of the lepton, that is, we take

$$\mathcal{A}^- = -\frac{1}{\sqrt{\eta}} \frac{x}{\tau_+ - \tau_-}, \quad (163)$$

$$\mathcal{B}^- = \frac{2\sqrt{\eta}}{\tau_+ - \tau_-}. \quad (164)$$

The factor Γ_0 is defined in Eq.(154), while

$$F_0^-(x, t) = \frac{(1 - \rho - x + t)}{\tau_+ - \tau_-} [\tau_+(x - t - \eta) - \eta(1 + \rho - t)] \quad (165)$$

and

$$F_{1,A}^-(x, t) = F_0^- \Phi_0 + \sum_{n=1}^5 D_n^A \Phi_n + D_6^A, \quad (166)$$

$$F_{1,B}^-(x, t) = F_0^- \Psi_0 + \sum_{n=1}^5 D_n^B \Psi_n + D_6^B. \quad (167)$$

The factor 12 in the formula (162) is introduced to meet the widely used [35, 45, 59] convention for $F_0(x)$ and Γ_0 . The symbols present in (166) are defined as follows:

$$\begin{aligned} \Phi_0 = & \frac{2p_0}{p_3} [Li_2\left(1 - \frac{1 - \tau^+}{p_+}\right) + Li_2\left(1 - \frac{1 - t/\tau^+}{p_+}\right) \\ & - Li_2\left(1 - \frac{1 - \tau^+}{p_-}\right) - Li_2\left(1 - \frac{1 - t/\tau^+}{p_-}\right) \\ & + Li_2(w_-) - Li_2(w_+) + 4Y_p \ln \sqrt{\rho}] \\ & + 4\left(1 - \frac{p_0}{p_3} Y_p\right) \ln(z_{max} - \rho) - 4 \ln z_{max}, \end{aligned} \quad (168)$$

$$\Phi_1 = Li_2(w_-) + Li_2(w_+) - Li_2(\tau_+) - Li_2(t/\tau_+) \quad (169)$$

$$\Phi_2 = \frac{Y_p}{p_3}, \quad (170)$$

$$\Phi_3 = \frac{1}{2} \ln \sqrt{\rho}, \quad (171)$$

$$\Phi_4 = \frac{1}{2} \ln(1 - \tau_+), \quad (172)$$

$$\Phi_5 = \frac{1}{2} \ln(1 - t/\tau_+), \quad (173)$$

$$\begin{aligned} \Psi_0 = & 4\left(\frac{p_0}{p_3} Y_p - 1\right) \ln\left(\frac{z_{max} - \rho}{z_{min} - \rho}\right) + 4 \ln\left(\frac{z_{max}}{z_{min}}\right) \\ & + \frac{2p_0}{p_3} [Li_2\left(1 - \frac{1 - \tau_+}{p_-}\right) + Li_2\left(1 - \frac{1 - t/\tau_+}{p_-}\right) \\ & - Li_2\left(1 - \frac{1 - \tau_+}{p_+}\right) - Li_2\left(1 - \frac{1 - t/\tau_+}{p_+}\right) \\ & + Li_2\left(1 - \frac{1 - \tau_-}{p_+}\right) + Li_2\left(1 - \frac{1 - t/\tau_-}{p_+}\right) \\ & - Li_2\left(1 - \frac{1 - \tau_-}{p_-}\right) - Li_2\left(1 - \frac{1 - t/\tau_-}{p_-}\right)], \end{aligned} \quad (174)$$

$$\Psi_1 = Li_2(\tau_+) + Li_2(t/\tau_+) - Li_2(\tau_-) - Li_2(t/\tau_-), \quad (175)$$

$$\Psi_2 = \frac{1}{2} \ln(1 - \tau_-), \quad (176)$$

$$\Psi_3 = \frac{1}{2} \ln(1 - t/\tau_-), \quad (177)$$

$$\Psi_4 = \frac{1}{2} \ln(1 - \tau_+), \quad (178)$$

$$\Psi_5 = \frac{1}{2} \ln(1 - t/\tau_+). \quad (179)$$

We introduce $C_1 \dots C_5$ to simplify the formulae for D_n^A and D_n^B :

$$\begin{aligned} C_1 &= \frac{1}{\sqrt{x^2 - 4\eta}} [\rho(-\eta x + 4\eta t - \eta\tau_+ - 4\eta + x\tau_+ - t\tau_+) - 2\rho^2\eta + \eta(xt + x \\ &\quad + 4t - 2t^2 + 6 + 2\eta) + \tau_+(-\eta x + \eta t + 5\eta - 2xt + x + t + t^2)]; \end{aligned} \quad (180)$$

$$\begin{aligned} C_2 &= \rho(\eta - t - 2\tau_+) + (xt^2 - 2t^2\tau_+)/(2\eta) + \eta(-x - 2t + 2\tau_+ + 30)/2 \\ &\quad + t(1 + t - x) + \tau_+(-2x + 2t + 6); \end{aligned} \quad (181)$$

$$\begin{aligned} C_3 &= \frac{1}{\sqrt{x^2 - 4\eta}} [\rho(-10\eta x + 18\eta t - 7\eta\tau_+ + xt + 7x\tau_+ - 11t\tau_+ + 4\tau_+) \\ &\quad + \rho^2(-9\eta + \tau_+) + (2xt^2\tau_+ - x^2t^2/2 - t^2\tau_+^2)/\eta + \eta^2(-\tau_+ + 10) \\ &\quad + xt(x - t - 1)\eta(4xt - x\tau_+ - 2x - x^2/2 + t\tau_+ + 4t \\ &\quad - 4t^2 + 11\tau_+ - \tau_+^2 - 12) + \tau_+(-6xt - x + 2x^2 - 3t + 5t^2 - 5)]; \end{aligned} \quad (182)$$

$$\begin{aligned} C_4 &= \frac{1}{\sqrt{x^2 - 4\eta}} [\rho(2\eta x\tau_+/t - 8\eta x + 8\eta\tau_+/t + 18\eta t - 11\eta\tau_+ - 4\eta^2\tau_+/t^2 \\ &\quad - xt + 5\tau_+x - 7t\tau_+) + \rho^2(2\eta\tau_+/t - 9\eta - \eta^2\tau_+/t^2) + xt(1 + t - x) \\ &\quad + (-2xt^2\tau_+ + x^2t^2/2 + t^2\tau_+^2)/\eta + \eta^2(5\tau_+/t^2 - 6\tau_+/t - 16/t + 6) \\ &\quad + \eta(2x\tau_+/t + 2xt - 3x\tau_+ - 4x + x^2/2 - 10\tau_+/t + 3t\tau_+ + 12t \\ &\quad - 4t^2 + 3\tau_+ + \tau_+^2 + 4) + \tau_+(-4xt - 3x + 2x^2 + 11t + 2t^2)]; \end{aligned} \quad (183)$$

$$\begin{aligned} C_5 &= [\rho/(x - t - \eta/t)](-\rho\eta^2\tau_+/t^2 + \eta\tau_+/t - \eta - \eta^2\tau_+/t^2 + \eta^2/t + \rho\eta\tau_+/t \\ &\quad - \rho\eta + \rho\eta^2/t)/2 + [\rho/(1 - x + \eta)](-\eta t - \eta\tau_+ + \eta^2 + t\tau_+)/2 \\ &\quad + \rho(3\eta\tau_+/t + 9\eta - 9t - 3\tau_+)/2 + (xt^2/4 - t^2\tau_+)/\eta + \eta(3x - 10\tau_+/t \\ &\quad - 12t - 2\tau_+ - 24 + 2\eta)/4 + (3t + 5)\tau_+/2 - xt + 6t + 5t^2/2]; \end{aligned} \quad (184)$$

$$D_1^A = C_1; \quad (185)$$

$$\begin{aligned} D_2^A &= \frac{1}{4\sqrt{x^2 - 4\eta}} \{ \rho\eta(34 - 6x\tau_+/t^2 - 4x/t^2 + 3x/t + 5xt - 2x\tau_+ + 2x \\ &\quad + 3x^2/t^2 + x^2 + 8\tau_+/t^2 + 18\tau_+/t - 2/t + 2t\tau_+ + 38t - 14t^2 + 20\tau_+) \\ &\quad + \rho\eta^2(16 - 2x/t^2 - 5\tau_+/t^2 - 2\tau_+/t + 16/t - \tau_+) + \rho\tau_+(-4xt - 4x + 6t \\ &\quad + 7t^2 + 11) + \rho^2 [\eta(-10 + 6x\tau_+/t^2 + 6x/t^2 + 4x\tau_+/t - 3x - 3x^2/t^2 \\ &\quad - 2x^2/t - 12\tau_+/t^2 - 18\tau_+/t + 6/t + 18t - 6\tau_+) + \eta^2(x/t^2 + \tau_+/t^2 \\ &\quad - \tau_+/t - 2/t) + \tau_+(2x - 5t - 7) + \rho\eta(-10 - 2x\tau_+/t^2 - 4x/t^2 - x/t \\ &\quad + x^2/t^2 + 8\tau_+/t^2 + 6\tau_+/t - 6/t) + \rho\eta^2\tau_+/t^2 + \rho\tau_+ + \rho^2\eta(x/t^2 - 2\tau_+/t^2 \\ &\quad + 2/t)] + \tau_+(-4xt + 2xt^2 + 2x + 7t + t^2 - 3t^3 - 5) + \eta(-14 + 2x\tau_+/t^2 \\ &\quad + x/t^2 - 4x\tau_+/t - 2x/t + 4xt - 2xt^2 + 2x\tau_+ - x - x^2/t^2 + 2x^2/t - x^2 \\ &\quad - 2\tau_+/t^2 - 6\tau_+/t - 10t\tau_+ + 32t - 22t^2 + 4t^3 + 18\tau_+) + \eta^2(28 + x/t^2 \\ &\quad - 2x/t + x + 3\tau_+/t^2 - 5\tau_+/t - 14/t + t\tau_+ - 14t + \tau_+); \end{aligned} \quad (186)$$

$$D_4^A = -C_3 - C_2; \quad (188)$$

$$D_5^A = -C_4 + C_2; \quad (189)$$

$$\begin{aligned}
D_6^A &= -\frac{1}{2}C_5 + \frac{1}{4\sqrt{x^2 - 4\eta}} \left\{ [\rho/(1-x+\eta)] [\eta(t\tau_+ + t + \tau_+) - \eta^2(1+t+\tau_+ + \right. \right. \\
&\quad \left. \left. + \eta^3 - t\tau_+)\right] + [\rho/(x-t-\eta/t)](1+\rho) [\eta(t-\tau_+) + \eta^2(-1+\tau_+/t^2 + \right. \right. \\
&\quad \left. \left. \tau_+/t - 1/t) + \eta^3(1/t^2 - \tau_+/t^3)\right] + \rho\eta(43 - x\tau_+/t - 4x/t - 5x + 2x^2/t \\
&\quad + 9\tau_+/t + 13t + 5\tau_+) + \rho\eta^2(-5 - \tau_+/t^2 + 2\tau_+/t + 1/t) + \tau_+(9xt + 5x \\
&\quad + 4t - 6t^2) + 12xt + 5xt^2 - 2x^2t + \rho(-9xt - 3x\tau_+ + 5t\tau_+) + \\
&\quad \rho^2\eta(-10 + 2x/t - 3\tau_+/t) + \rho^2\eta^2(-\tau_+/t^2 + 1/t) + (-6xt^2\tau_+ + x^2t^2 \\
&\quad + 2t^2\tau_+^2)/(2\eta) + \eta(-35 - x\tau_+/t + 2x/t - 2xt + 4x\tau_+ + 26x \\
&\quad - 2x^2/t - 3x^2/2 - 4\tau_+/t - 2t\tau_+ - 34t - t^2 - 22\tau_+ - 3\tau_+^2) \\
&\quad \left. + \eta^2(-2 + 2x/t - x + 6\tau_+/t + 2t)\right\}; \quad (190)
\end{aligned}$$

$$D_1^B = C_1 \quad (191)$$

$$D_2^B = C_2 - C_3 \quad (192)$$

$$D_3^B = -C_2 - C_4 \quad (193)$$

$$D_4^B = C_2 + C_3 \quad (194)$$

$$D_5^B = -C_2 + C_4 \quad (195)$$

$$D_6^B = C_5 \quad (196)$$

(197)

One can perform the limit $\rho \rightarrow 0$, which corresponds to the decay of the bottom quark to an up quark and leptons. The formulae, which are much simpler in this case, are presented in the same manner as the full results:

$$\frac{d\tilde{\Gamma}^-}{dx dt} = \begin{cases} 12\Gamma_0 \left[\tilde{F}_0^-(x, t) - \frac{2\alpha_s}{3\pi} \tilde{F}_{1,A}^-(x, t) \right] & \text{for (x, t) in A} \\ 12\Gamma_0 \frac{2\alpha_s}{3\pi} \tilde{F}_{1,B}^-(x, t) & \text{for (x, t) in B} \end{cases} \quad (198)$$

with

$$\tilde{F}_0^-(x, t) = \frac{(1-x-t)}{\tau_+ - \tau_-} [\tau_+(x-t-\eta) - \eta(1-t)] \quad (199)$$

and

$$\tilde{F}_{1,A}^-(x, t) = \tilde{F}_0 \tilde{\Phi}_0 + \sum_{n=1}^5 \mathcal{D}_n^A \tilde{\Phi}_n + \mathcal{D}_6^A, \quad (200)$$

$$\tilde{F}_{1,B}^-(x, t) = \tilde{F}_0 \tilde{\Psi}_0 + \sum_{n=1}^5 \mathcal{D}_n^B \tilde{\Psi}_n + \mathcal{D}_6^B. \quad (201)$$

where

$$\begin{aligned} \tilde{\Phi}_0 = 2 & \left[Li_2\left(\frac{\tau_+ - t}{1 - t}\right) + Li_2\left(\frac{1/\tau_+ - 1}{1/t - 1}\right) + Li_2(t) \right] + \frac{1}{2}\pi^2 \\ & + \ln^2(1 - \tau_+) \ln^2(1 - t) + \ln^2(1 - t/\tau_+) \\ & - 2 \ln(1 - t) \ln z_{max}, \end{aligned} \quad (202)$$

$$\tilde{\Phi}_1 = \frac{\pi^2}{12} + Li_2(t) - Li_2(\tau_+) - Li_2(t/\tau_+),$$

$$\tilde{\Phi}_{2 \diamond 3} = \frac{2 \ln(1 - t)}{1 - t}, \quad (203)$$

$$\tilde{\Phi}_4 = \Phi_4, \quad (204)$$

$$\tilde{\Phi}_5 = \Phi_5, \quad (205)$$

and

$$\begin{aligned} \tilde{\Psi}_0 = 2 & \left[Li_2\left(\frac{\tau_+ - t}{1 - t}\right) + Li_2\left(\frac{1/\tau_- - 1}{1/t - 1}\right) - Li_2\left(\frac{\tau_+ - t}{1 - t}\right) \right. \\ & \left. - Li_2\left(\frac{1/\tau_+ - 1}{1/t - 1}\right) \right] + \ln(1 - t) \ln\left(\frac{z_{max}}{z_{min}}\right) \\ & - \ln\left(\frac{1 - \tau_+}{1 - \tau_-}\right) \ln[(1 - \tau_+)(1 - \tau_-)] \\ & - \ln\left(\frac{1 - t/\tau_+}{1 - t/\tau_-}\right) \ln[(1 - t/\tau_+)(1 - t/\tau_-)], \end{aligned} \quad (206)$$

$$\tilde{\Psi}_n = \Psi_n, \quad (n = 1 \dots 5). \quad (207)$$

$$\begin{aligned} \mathcal{C}_1^A = & \frac{1}{\sqrt{x^2 - 4\eta}} \left[\eta(6 + xt - x\tau_+ + x + t\tau_+ + 4t - 2t^2 + 5\tau_+) + 2\eta^2 + \right. \\ & \left. \tau_+(x - 2xt + t + t^2) \right]; \end{aligned} \quad (208)$$

$$\begin{aligned} \mathcal{C}_2^A = & (xt^2 - 2t^2\tau_+)/(2\eta) + \eta(30 - x - 2t + 2\tau_+)/2 - xt - 2x\tau_+ + 2t\tau_+ \\ & + t + t^2 + 6\tau_+; \end{aligned} \quad (209)$$

$$\begin{aligned} \mathcal{C}_3^A = & \frac{1}{\sqrt{x^2 - 4\eta}} \left[(4xt^2\tau_+ - x^2t^2 - 2t^2\tau_+^2)/(2\eta) + \eta^2(10 - \tau_+) \right. \\ & \left. \eta(-24 + 8xt - 2x\tau_+ - 4x - x^2 + 2t\tau_+ + 8t - 8t^2 + 22\tau_+ - 2\tau_+^2)/2 \right] \end{aligned}$$

$$-6xt\tau_+ - xt - xt^2 - x\tau_+ + x^2t + 2x^2\tau_+ - 3t\tau_+ + 5t^2\tau_+ - 5\tau_+] ; \quad (210)$$

$$\begin{aligned} \mathcal{C}_4^A &= \frac{1}{\sqrt{x^2 - 4\eta}} [(-4xt^2\tau_+ + x^2t^2 + 2t^2\tau_+^2)/(2\eta) + \eta(4 + 2x\tau_+/t + 2xt \\ &\quad - 3x\tau_+ - 4x + x^2/2 - 10\tau_+/t + 3t\tau_+ + 12t - 4t^2 + 3\tau_+ + \tau_+^2) \\ &\quad + \eta^2(6 + 5\tau_+/t^2 - 6\tau_+/t - 16/t) - 4xt\tau_+ + xt + xt^2 - 3x\tau_+ \\ &\quad - x^2t + 2x^2\tau_+ + 11t\tau_+ + 2t^2\tau_+] ; \end{aligned} \quad (211)$$

$$\begin{aligned} \mathcal{C}_5^A &= (xt^2 - 4t^2\tau_+)/(4\eta) + \eta(-24 + 3x - 10\tau_+/t - 12t - 2\tau_+)/4 \\ &\quad + \eta^2/2 - xt + 3t\tau_+/2 + 6t + 5t^2/2 + 5\tau_+/2; \end{aligned} \quad (212)$$

$$\mathcal{D}_1^A = \mathcal{C}_1 \quad (213)$$

$$\begin{aligned} \mathcal{D}_{2\circ 3}^A &= \frac{1}{4\sqrt{x^2 - 4\eta}} [\eta(-14 + 2x\tau_+/t^2 + x/t^2 - 4x\tau_+/t - 2x/t + 4xt - 2xt^2 \\ &\quad + 2x\tau_+ - x - x^2/t^2 + 2x^2/t - x^2 - 2\tau_+/t^2 - 6\tau_+/t - 10t\tau_+ + 32t \\ &\quad - 22t^2 + 4t^3 + 18\tau_+) + \eta^2(28 + x/t^2 - 2x/t + x + 3\tau_+/t^2 - 5\tau_+/t \\ &\quad - 14/t + t\tau_+ - 14t + \tau_+) + (-4xt\tau_+ + 2xt^2\tau_+ + 2x\tau_+ + 7t\tau_+ + t^2\tau_+ \\ &\quad - 3t^3\tau_+ - 5\tau_+)] ; \end{aligned} \quad (214)$$

$$\mathcal{D}_4^A = -\mathcal{C}_2 - \mathcal{C}_3, \quad (215)$$

$$\mathcal{D}_5^A = \mathcal{C}_2 - \mathcal{C}_4, \quad (216)$$

$$\begin{aligned} \mathcal{D}_6^A &= -\frac{1}{2}\mathcal{C}_5 + \frac{1}{4\sqrt{x^2 - 4\eta}} [(-6xt^2\tau_+ + x^2t^2 + 2t^2\tau_+^2)/(2\eta) \\ &\quad + \eta(-35 - x\tau_+/t + 2x/t - 2xt + 4x\tau_+ + 26x - 2x^2/t - 3x^2/2 - 4\tau_+/t \\ &\quad - 2t\tau_+ - 34t - t^2 - 22\tau_+ - 3\tau_+^2) + \eta^2(-2 + 2x/t - x + 6\tau_+/t + 2t) \\ &\quad + (9xt\tau_+ + 12xt + 5xt^2 + 5x\tau_+ - 2x^2t + 4t\tau_+ - 6t^2\tau_+)] ; \end{aligned} \quad (217)$$

On integration over t , one obtains tau energy distributions according to the formula

$$\frac{1}{12\Gamma_0} \frac{d\Gamma^-}{dx} = f_0^-(x) - \frac{2\alpha_s}{3\pi} f_1^-(x). \quad (218)$$

where if we drop the superscript '−' we obtain the corresponding formula for the unpolarized case.

The results are presented in Fig. 18, where the polarisation is plotted versus the τ lepton energy. Both the Born and first order approximation are showed. In order to make the correction more explicit, we also present another diagram, where the function $R(x)$ is drawn, defined as following:

$$1 - P(x) = [1 - P_0(x)][1 + \frac{2\alpha_s}{3\pi} R(x)] \quad (219)$$

which gives the expression for $R(x)$:

$$R(x) = \frac{f_1(x)}{f_0(x)} - \frac{f_1^-(x)}{f_0^-(x)}, \quad (220)$$

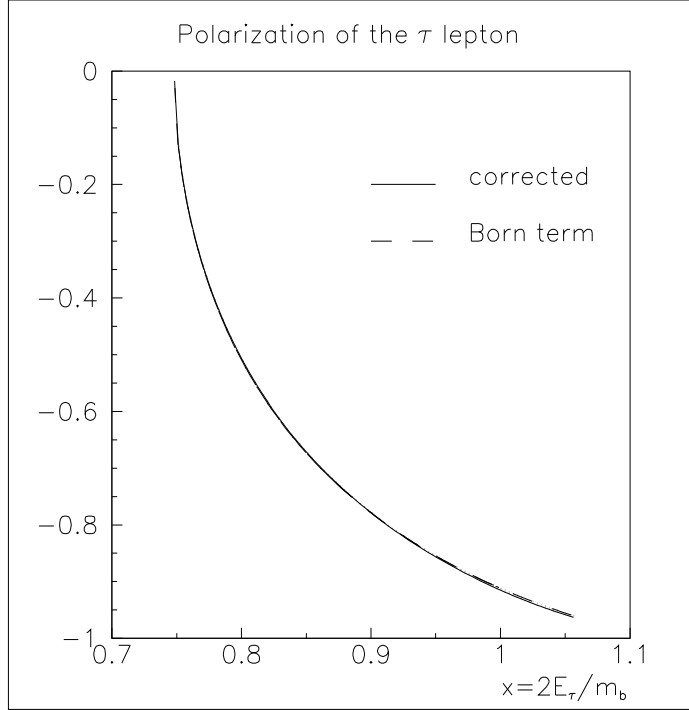


Figure 18: Polarisation of τ lepton in the Born approximation (dashed line) and including the first order QCD correction (solid line) as functions of the scaled τ energy x . The mass of the b quark taken at 4.75 GeV, c quark 1.35 GeV and the coupling constant $\alpha_s = 0.2$

thus its meaning is how the radiative corrections differ with respect to the state of polarisation they act on. In (219) P_0 denotes the zeroth order approximation to the polarisation. The function $f_1^-(x)/f_0^-(x)$ has been presented in Fig. 19, while Fig. 20 shows the function $R(x)$, so that one can immediately see how small the correction is in comparison to the correction to the energy distribution.

Integrating over the charged lepton energy one can obtain its total polarisation as well as the corrections to which it is subject. If we take $m_b = 4.75$ GeV as the central value for the decaying quark mass and $m_b = 4.4$ and $m_b = 5.2$ for the limits, we arrive at the following (the mass difference $m_b - m_c = 3.4$ GeV everywhere):

$$1 - P = (1 - P_0) \left(1 + \frac{2\alpha_s}{3\pi} R_s + \frac{\lambda_1^2}{m_b^2} R_{np}^1 + \frac{\lambda_2^2}{m_b^2} R_{np}^2 \right) \quad (221)$$

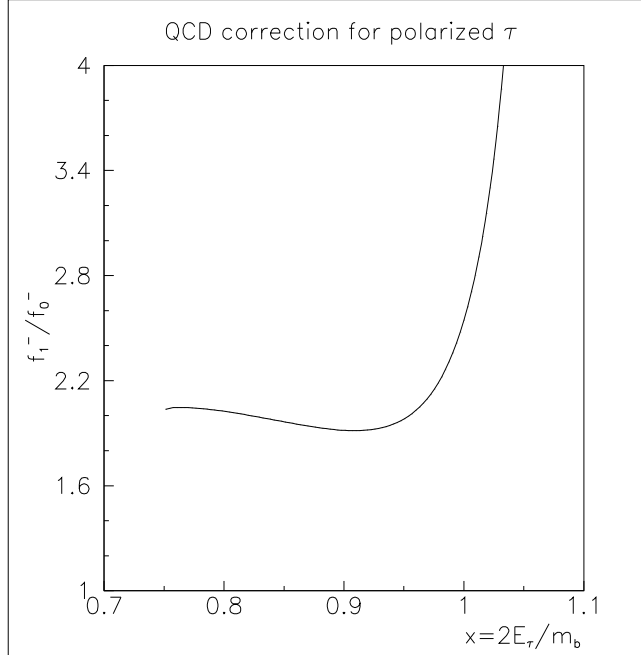


Figure 19: The ratio $f_1^-(x)/f_0^-(x)$ representing the radiative correction for the negatively polarized state as dependent on the scaled τ lepton energy x .

with

$$\begin{aligned}
 P_0 &= -0.7388_{-0.0109}^{+0.0105} \\
 R_s &= -0.016_{-0.017}^{+0.023} \\
 R_{np}^1 &= 0.421_{-0.025}^{+0.027} \\
 R_{np}^2 &= -2.28_{-0.16}^{+0.22}
 \end{aligned}$$

6.4 Moments of τ energy distribution

The moments of τ energy distribution, which are useful sources of information on the physical parameters regarding the discussed decay can be evaluated according to the formula:

$$M_n^\pm = \int_{E_{min}}^{E_{max}} E_\tau^n \frac{d\Gamma^\pm}{dE_\tau} dE_\tau, \quad (222)$$

$$r_n^\pm = \frac{M_n^\pm}{M_0^\pm}, \quad (223)$$

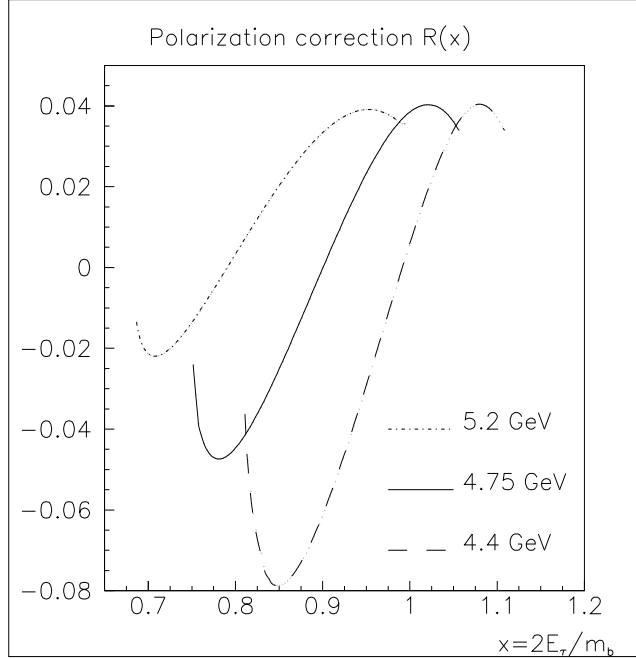


Figure 20: The QCD-correction function $R(x)$ for the pole mass values of the b quark taken to be 4.4 GeV (dashed), 4.75 GeV (solid) and 5.2 GeV (dash-dotted) as dependent on the scaled τ lepton energy x .

where E_{min} and E_{max} are the lower and upper limits for τ energy and M_n include both perturbative and nonperturbative QCD corrections to τ energy spectrum. The superscripts denote the polarisation states. Since one obviously has

$$M_n = M_n^+ + M_n^- \quad (224)$$

where M_n stands for the unpolarized momenta, we only give the values of the momenta for the negative polarisation case. The unpolarized distributions were given in [36, 37]. The nonperturbative corrections to the charged lepton spectrum from semileptonic B decay have been derived in the HQET framework up to order of $1/m_b^2$ [42, 43, 44, 45]. The corrected heavy lepton energy spectrum can be written in the following way:

$$\frac{1}{12\Gamma_0} \frac{d\Gamma}{dx} = f_0(x) - \frac{2\alpha_s}{3\pi} f_1(x) + \frac{\lambda_1}{m_b^2} f_{np}^{(1)}(x) + \frac{\lambda_2}{m_b^2} f_{np}^{(2)}(x), \quad (225)$$

where λ_1 and λ_2 are the HQET parameters corresponding to the b quark kinetic energy and the energy of interaction of the b quark magnetic moment with the chromomagnetic field produced by the light quark in the meson B . The

functions $f_{np}^{(1,2)}$ can be easily extracted from the formula (2.11) in [45]. The formula (225) looks identically if one considers definite polarisation state of the final τ lepton. The appropriate calculation within the HQET scheme has also been performed [45], see formula (2.12) therein.

Following ref.[59] we expand the ratios r_n :

$$r_n^- = r_n^{(0)-} \left(1 - \frac{2\alpha_s}{3\pi} \delta_n^{(p)-} + \frac{\lambda_1}{m_b^2} \delta_n^{(1)-} + \frac{\lambda_2}{m_b^2} \delta_n^{(2)-} \right), \quad (226)$$

where $r_n^{(0)}$ is the lowest approximation of r_n ,

$$r_n^{(0)-} = \left(\frac{m_b}{2} \right)^n \frac{\int_{2\sqrt{\eta}}^{1+\eta-\rho} f_0^-(x) x^n dx}{\int_{2\sqrt{\eta}}^{1+\eta-\rho} f_0^-(x) dx}. \quad (227)$$

Each of the $\delta_n^{(i)-}$ is expressed by integrals of the corresponding correction function $f^{(i)}(x)$ and the tree level term $f_0(x)$

$$\delta_n^{(i)-} = \frac{\int_{2\sqrt{\eta}}^{1+\eta-\rho} f^{(i)-}(x) x^n dx}{\int_{2\sqrt{\eta}}^{1+\eta-\rho} f_0^-(x) x^n dx} - \frac{\int_{2\sqrt{\eta}}^{1+\eta-\rho} f^{(i)-}(x) dx}{\int_{2\sqrt{\eta}}^{1+\eta-\rho} f_0^-(x) dx}, \quad (228)$$

where the index i denotes any of the three kinds of corrections discussed above. The coefficients $\delta_n^{(i)}$ depend only on the two ratios of the charged lepton and the c quark to the mass m_b . Following ref.[36, 37] we employ the functional dependence of the form

$$\delta_n^{(i)-}(m_b, m_c, m_\tau) = \delta_n^{(i)-} \left(\frac{m_b}{m_\tau}, \frac{m_c}{m_b} \right). \quad (229)$$

The quark masses are not known precisely so we have calculated the coefficients in a reasonable range of the parameters, that is, $4.4 \text{ GeV} \leq m_b \leq 5.2 \text{ GeV}$ and $0.25 \leq m_c/m_b \leq 0.35$ and then fitted to them functions of the following form:

$$\begin{aligned} \delta(p, q) &= a + b(p - p_0) + c(q - q_0) + d(p - p_0)^2 \\ &= +e(p - p_0)(q - q_0) + f(q - q_0)^2, \end{aligned} \quad (230)$$

where $p = m_b/m_\tau$, $p_0 = 4.75 \text{ GeV}/1.777 \text{ GeV} = 2.6730$, $q = m_c/m_b$, $q_0 = 0.28$ and the polynomial coefficients can be fitted for each of the $\delta_n^{(i)}$ separately with a relative error of less than 2%. Our choice of the central values reflects the realistic masses of quarks: $m_b = 4.75 \text{ GeV}$ and $m_c = 1.35 \text{ GeV}$, for which $\delta_n^{(i)} = a_n^{(i)}$.

To bring out the difference in the extent to which the corrections affect the two different polarisation states it is useful to compare these coefficients with the ones obtained with the polarisation summed over. This can be done along the lines suggested by the treatment of the polarisation itself, see Eq.(219). The

corresponding expansion takes the form

$$\frac{r_n^-}{r_n^{(0)}} = \frac{r_n^{-(0)}}{r_n^{(0)}} \left[1 - \frac{2\alpha_s}{3\pi} (\delta_n^{(p)-} - \delta_n^{(p)}) + \frac{\lambda_1}{m_b^2} (\delta_n^{(1)-} - \delta_n^{(1)}) + \frac{\lambda_2}{m_b^2} (\delta_n^{(2)-} - \delta_n^{(2)}) \right]. \quad (231)$$

With these, one can readily find the actual relative correction of each kind, assuming reasonable values of α_s , λ_1 and λ_2 . Here we take $\alpha_s = 0.2, 0.15 \text{ GeV}^2 \leq -\lambda_1 \leq 0.60 \text{ GeV}^2$, $\lambda_2 = 0.12 \text{ GeV}^2$, keep the b quark mass fixed at 4.75 GeV and the mass of the c quark equal to 1.35 GeV. The corrections then read for $n = 1 (n = 5)$

Type	Correction to	
	$r_n^-/r_n^{(0)-}$	$r_n/r_n^{(0)}$
perturbative	$-0.00084(-0.0048)$	$-0.0009(-0.0052)$
kinetic energy	$0.008 \pm 0.005(0.06 \pm 0.04)$	$0.008 \pm 0.005(0.06 \pm 0.04)$
chromomagnetic	$-0.0097(-0.053)$	$-0.0092(-0.0511)$

6.5 Summary

We have calculated the one-loop QCD corrections to the longitudinal polarisation of the τ lepton in semileptonic B decays. This calculation has been published in [49]. As was expected from earlier results [35], the effect of the correction on the polarisation is negligible, which makes it a promising quantity for the determination of the quark masses. Discussing the moments of the lepton energy distribution, we have also included the nonperturbative corrections.

7 Polarisation of τ lepton with respect to W

7.1 Introduction

The method used in the calculation of the longitudinal polarisation can easily be modified to give other polarisations. This fact matters insomuch that experimentally it is the polarisation along the intermediating W boson direction that is easier to measure [46], see also [47]. The reason is that the direction of τ lepton can be determined at B factories with rather poor accuracy. On the other hand the direction of W is opposite to the direction of hadrons in semileptonic B decays. The latter can be well measured at least for the exclusive $B \rightarrow D\tau\bar{\nu}_\tau$ and $B \rightarrow D^*\tau\bar{\nu}_\tau$ channels which probably contribute the dominant contribution to the inclusive decay rate.

In the calculation below, we find the tree level term and the $\mathcal{O}(1/m_b^2)$ HQET corrections to the doubly differential rate with the final τ lepton polarized along the momentum of the intermediate W boson. The one-loop correction is presented in a plot as it has been evaluated numerically. Also we give the tree level charged lepton distribution in an analytic form.

The HQET mass power corrections to the lepton spectra in semileptonic B decays have been applied to the calculation of the polarisation of the lepton. The mass of the lepton had of course to be taken into account, which was done for unpolarised distributions in [42, 43]. The kinematical complications arising due to the massive lepton are also discussed therein. The longitudinal polarisation was calculated in [45]. Some further problems emerged in the calculation of the corrections to the transverse polarisations found in [48]. The case we consider leads to apparent divergences, but they cancel so that no special regularisation has to be employed.

After a brief note on the kinematics in Sec. 7.2 we discuss the way the polarisation is evaluated, Sec. 7.3. An analytic formula for the double differential distribution is presented including the mass power corrections in Sec. 7.4. Due to its complicated form, we only show numerical form of the lepton energy distribution in Sec. 7.5. This section contains also the one-loop perturbative corrections. All of these corrections are presented in a plot. Finally we summarize the results.

7.2 Kinematics

Recall that the phase space is defined by the ranges of the kinematical variables:

$$2\sqrt{\eta} \leq x \leq 1 + \eta - \rho = x_m , \quad (232)$$

$$t_{min} = \tau_- \left(1 - \frac{\rho}{1 - \tau_-} \right) \leq t \leq \tau_+ \left(1 - \frac{\rho}{1 - \tau_+} \right) = t_{max} . \quad (233)$$

The limits above are obtained within the parton model approximation. They change if we allow for Fermi motion, which we must in order to be able to discuss the HQET corrections to the decay widths[42, 45, 43, 44, 48, 41]. Also, contrary to the parton model case, the energy of neutrino can vary within limits

which depend in a non-trivial manner on the values of the variables x, t . The details of the subject were discussed in [42], so we will only state here that the integrations involving delta functions and their derivatives have the effect of confining the range of the variables x, t to that of the parton model. This is easily seen from the form of the corrections, see Eq.(52).

7.3 Polarisation evaluation

The polarisation is found by evaluating the unpolarized decay width and any of the two corresponding to a definite polarisation, according to the definition,

$$P = \frac{\Gamma^+ - \Gamma^-}{\Gamma^+ + \Gamma^-} = 1 - 2 \frac{\Gamma^-}{\Gamma} \quad , \quad (234)$$

where $\Gamma = \Gamma^+ + \Gamma^-$. In this calculation we follow the method employed when dealing with the longitudinal polarisation of the charged lepton. Thus in the rest frame of the decaying quark, one can decompose:

$$s = \mathcal{A}Q + \mathcal{B}W \quad . \quad (235)$$

The coefficients \mathcal{A}, \mathcal{B} can be evaluated using the conditions defining the polarisation four-vector s , which reduce to the following when the parton model value of the neutrino energy is assumed:

$$\mathcal{A}_0^\pm = \mp \frac{t + \eta}{\sqrt{t(x - x_-)(x_+ - x)}} \quad , \quad (236)$$

$$\mathcal{B}_0^\pm = \pm \frac{x}{\sqrt{t(x - x_-)(x_+ - x)}} \quad , \quad (237)$$

where the superscripts at \mathcal{A}, \mathcal{B} denote the polarisation of the lepton, while

$$x_\pm = (1 + \eta/t)w_\pm \quad . \quad (238)$$

However, the coefficients in the decomposition (147) need to be re-evaluated, taking into account the Fermi motion and working in the rest frame of the decaying meson. We will presently construct the four-vector s representing a charged lepton polarized along the direction of the W boson. The defining properties of s are

$$s^2 = -1 \quad (239)$$

and

$$s \cdot \tau = 0 \quad , \quad (240)$$

complemented by the relation $\vec{s} \parallel \vec{W}$. Since we are working in the rest frame of the decaying meson, the four-vector s can be decomposed as

$$s = \mathcal{A}v + \mathcal{B}W \quad , \quad (241)$$

where v and W stand for the four-velocity of the B meson and the four-momentum of the intermediate W boson, respectively. While this form automatically satisfies $\vec{s} \parallel \vec{W}$, the other two relations (239) and (240) have to be

imposed, hence yielding the expressions for the coefficients appearing in (241). With $v = (1, 0, 0, 0)$, one readily identifies:

$$v \cdot \tau = x/2, \quad v \cdot \nu = x_\nu/2, \quad v^2 = -1. \quad (242)$$

These combined with the other dot products lead to the following formulae:

$$\mathcal{A}_\pm = \frac{\mp(t + \eta)}{\sqrt{x(t + \eta)(x + x_\nu) - x^2t - (t + \eta)^2}} , \quad (243)$$

$$\mathcal{B}_\pm = \frac{\pm x}{\sqrt{x(t + \eta)(x + x_\nu) - x^2t - (t + \eta)^2}} . \quad (244)$$

The evaluation of the HQET corrections involves differentiation over the neutrino energy, once or twice. The denominator in the above expressions is easily seen to vanish at the point where the W boson is at rest. It is known that the kinematics of the process, together with the delta functions and their derivatives, finally reduces to integration over the partonic phase space. Then there is one such point where the denominator vanishes,

$$x = 1 - \sqrt{\rho} + \frac{\eta}{1 - \sqrt{\rho}} , \quad (245)$$

$$t = (1 - \sqrt{\rho})^2 . \quad (246)$$

One might thus raise the question of analyticity of the expressions obtained in this way. However, the divergences cancel and moreover the resulting distribution is continuous if we ignore the endpoint behaviour. That this is so indeed, may be verified by changing the variables from t to the square of the three-momentum of the W boson. Then the singularity makes its presence only on integration over w_3^2 rather than affecting the analytical structure of the distributions. It turns out that using this variable one obtains an analytic expression. This is made clear once one notices that the only terms that occur in the course of the calculation are the dot products of the four-vector s and the other four-vectors. Writing them out explicitly,

$$s_+ \cdot v = \frac{\tau_3 \cos \theta}{\sqrt{x^2 - \tau_3 \cos^2 \theta}} , \quad (247)$$

$$s_+ \cdot W = \frac{(x + x_\nu)\tau_3 \cos \theta - 2xw_3}{2\sqrt{x^2 - \tau_3 \cos^2 \theta}} , \quad (248)$$

with

$$\cos \theta = \frac{w_3^2 - \eta - (x_\nu - x)/4}{w_3 \tau_3} , \quad (249)$$

where the subscript denotes the polarisation direction, we easily verify that the triple differential distribution is analytic in the neutrino energy. Lastly, let us note that another change of variable can be useful for evaluating the distribution. Namely, using the cosine of the angle subtended by the tau lepton and the neutrino[48] eliminates the singular terms from the double differential

distribution. We have checked numerically that the resulting distribution is the same. Applying now the representation (235) of the polarisation four-vector s we obtain the following formula for the matrix element with the lepton polarized:

$$\mathcal{M}^\pm = \frac{1}{2} \mathcal{M}^{un}(\tau) \pm \frac{\sqrt{\eta}}{\sqrt{x(t+\eta)(x_\nu+x) - x^2t - (t+\eta)^2}} [x\mathcal{M}^{un}(W) - (t+\eta)\mathcal{M}^{un}(Q)] . \quad (250)$$

The above expression is valid for the HQET corrections, too. The first term on the right hand side of (250) can be calculated immediately once we know the result for the unpolarized case. Then the other terms require the formal replacement of the four-momenta $\tau \rightarrow W$ and $\tau \rightarrow Q$ in the argument.

7.4 Double differential distribution

The polarized distribution can be written in the form,

$$\frac{1}{\Gamma_0} \frac{d\Gamma^\pm}{dx dt} = \frac{1}{2} F^{un} \pm \left(\tilde{F} + \tilde{F}_+ - \tilde{F}_- \right) , \quad (251)$$

where

$$\Gamma_0 = \frac{G_F^2 m_b^5}{192\pi^3} |V_{CKM}|^2 . \quad (252)$$

The first term on the right hand side of Eq.(251) stands for the unpolarized distribution, given e.g. in [42], Eq.(30). Here we will only give the new other term:¹

$$\tilde{F} = \sqrt{\eta} \mathcal{W} [6f_1 + K_b \mathcal{W} (f_2 + f_3 \mathcal{W}^2 + \frac{3}{2} f_4 \mathcal{W}^4) + G_b (f_5 + f_6 \mathcal{W}^2)] \quad (253)$$

where

$$\begin{aligned} f_1 &= -xt(1+\rho-\eta) + 2xt^2 - x(1+\rho\eta-2\rho+\rho^2+\eta) - x^2t \\ &\quad + x^2(1-\rho) + t(1+2\rho\eta-\rho^2) + t^2(2\rho-\eta) - t^3 - \rho^2\eta + \eta , \end{aligned} \quad (254)$$

$$\begin{aligned} f_2 &= -8xt(1-\rho+\eta) - 16xt^2 + 8x(1+\rho\eta-2\rho+\rho^2-\eta) + 6x^2t \\ &\quad - 6x^2(1-\rho) + 2t(1-6\rho\eta-4\rho+3\rho^2+12\eta) + 2t^2(8-6\rho+3\eta) \\ &\quad + 6t^3 - 8\rho\eta + 6\rho^2\eta + 2\eta + 8\eta^2 , \end{aligned} \quad (255)$$

$$\begin{aligned} f_3 &= xt(-10\rho\eta+6\rho\eta^2+14\rho^2\eta+9\rho^2\eta^2-6\rho^3\eta+2\eta+9\eta^2-4\eta^3) \\ &\quad + xt^2(1-9\rho\eta^2-5\rho+18\rho^2\eta+7\rho^2-3\rho^3+6\eta-13\eta^2) \\ &\quad + xt^3(1-18\rho\eta-2\rho+9\rho^2-14\eta+3\eta^2) - xt^4(5+9\rho-6\eta) \\ &\quad + 3xt^5 + x(-5\rho\eta^2+4\rho\eta^3+7\rho^2\eta^2-3\rho^3\eta^2+\eta^2+4\eta^3) \\ &\quad + x^2t(1+14\rho\eta+2\rho\eta^2-3\rho-\rho^2\eta+3\rho^2-\rho^3-13\eta+8\eta^2) \\ &\quad + x^2t^2(-6+5\rho\eta+6\rho+15\eta-\eta^2) + x^2t^3(7+3\rho-3\eta) - 2x^2t^4 \end{aligned}$$

¹A FORTRAN code for this formula is available from piotr@charm.phys.us.edu.pl

$$\begin{aligned}
& + x^2\eta(-3\rho + 8\rho\eta + 3\rho^2 - \rho^2\eta - \rho^3 - 7\eta + 1) + x^3t(1 - \rho)^2 - x^3t^2\eta \\
& - x^3t^3 + x^3\eta(1 - \rho)^2,
\end{aligned} \tag{256}$$

$$\begin{aligned}
f_4 = & x^2t(-6\rho\eta^2 - 2\rho^2\eta^3 + 6\rho^3\eta^2 + 4\rho^3\eta^3 - 3\rho^4\eta^2 + 3\eta^2 - 2\eta^3) \\
& + x^2t^2(-6\rho\eta - 2\rho\eta^3 - 6\rho^2\eta^2 - 6\rho^2\eta^3 + 6\rho^3\eta + 12\rho^3\eta^2 - 3\rho^4\eta + 3\eta - 6\eta^2) \\
& + x^2t^3(1 - 6\rho\eta^2 + 4\rho\eta^3 - 2\rho - 6\rho^2\eta - 18\rho^2\eta^2 + 12\rho^3\eta + 2\rho^3 - \rho^4 - 6\eta + 2\eta^3) \\
& + x^2t^4(-2 - 6\rho\eta + 12\rho\eta^2 - 18\rho^2\eta - 2\rho^2 + 4\rho^3 + 6\eta^2 - \eta^3) \\
& + x^2t^5(12\rho\eta - 2\rho - 6\rho^2 + 6\eta - 3\eta^2) + x^2t^6(2 + 4\rho - 3\eta) - x^2t^7 \\
& + x^2(-2\rho\eta^3 + 2\rho^3\eta^3 - \rho^4\eta^3 + \eta^3) + x^3t(8\rho\eta + \rho\eta^2 + 2\rho\eta^3 - 12\rho^2\eta + \rho^2\eta^2 \\
& + 3\rho^2\eta^3 + 8\rho^3\eta - \rho^3\eta^2 - 2\rho^4\eta - 2\eta - \eta^2 + 3\eta^3) \\
& + x^3t^2(-1 - \rho\eta + 6\rho\eta^2 - 3\rho\eta^3 + 4\rho - \rho^2\eta + 9\rho^2\eta^2 - 6\rho^2 + \rho^3\eta + 4\rho^3 \\
& - \rho^4 + \eta + 9\eta^2 - 3\eta^3) \\
& + x^3t^3(1 + 6\rho\eta - 11\rho\eta^2 - \rho + 9\rho^2\eta - \rho^2 + \rho^3 + 9\eta - 11\eta^2 + \eta^3) \\
& + x^3t^4(3 - 13\rho\eta + 2\rho + 3\rho^2 - 13\eta + 4\eta^2) + x^3t^5(-5 - 5\rho + 5\eta) + 2x^3t^6 \\
& + x^3(4\rho\eta^2 + \rho\eta^3 - 6\rho^2\eta^2 + \rho^2\eta^3 + 4\rho^3\eta^2 - \rho^3\eta^3 - \rho^4\eta^2 - \eta^2 - \eta^3) \\
& + x^4t(-6\rho\eta + 2\rho\eta^2 + 6\rho^2\eta + \rho^2\eta^2 - 2\rho^3\eta + 2\eta - 3\eta^2) \\
& + x^4t^2(1 + 4\rho\eta + \rho\eta^2 - 3\rho + 2\rho^2\eta + 3\rho^2 - \rho^3 - 6\eta + 3\eta^2) \\
& + x^4t^3(-3 + 2\rho\eta + 2\rho + \rho^2 + 6\eta - \eta^2) + x^4t^4(3 + \rho - 2\eta) \\
& - x^4t^5 + x^4(-3\rho\eta^2 + 3\rho^2\eta^2 - \rho^3\eta^2 + \eta^2),
\end{aligned} \tag{257}$$

$$\begin{aligned}
f_5 = & 4xt(3 + 5\rho - 5\eta) - 40xt^2 + 4x(1 + 5\rho\eta - 6\rho + 5\rho^2 + \eta) + 10x^2t \\
& - 2x^2(1 - 5\rho) - 6t(1 + 10\rho\eta - 5\rho^2) - 2t^2(4 + 30\rho - 15\eta) + 30t^3 \\
& + 30\rho^2\eta - 6\eta + 8\eta^2,
\end{aligned} \tag{258}$$

$$\begin{aligned}
f_6 = & xt(-18\rho\eta - 2\rho\eta^2 + 6\rho^2\eta - 15\rho^2\eta^2 + 10\rho^3\eta + 2\eta + 17\eta^2 - 4\eta^3) \\
& + xt^2(1 - 16\rho\eta + 15\rho\eta^2 - 9\rho - 30\rho^2\eta + 3\rho^2 + 5\rho^3 + 10\eta - \eta^2) \\
& + xt^3(1 + 30\rho\eta - 10\rho - 15\rho^2 + 10\eta - 5\eta^2) + xt^4(7 + 15\rho - 10\eta) \\
& - 5xt^5 + x(-9\rho\eta^2 + 4\rho\eta^3 + 3\rho^2\eta^2 + 5\rho^3\eta^2 + \eta^2 + 8\eta^3) \\
& + x^2t(-1 + 30\rho\eta - 10\rho\eta^2 + 7\rho + 5\rho^2\eta - 11\rho^2 + 5\rho^3 - 11\eta - 4\eta^2) \\
& + x^2t^2(-2 - 25\rho\eta + 18\rho - 19\eta + 5\eta^2) - 15x^2t^3(1 + \rho - \eta) \\
& + 10x^2t^4 + x^2(7\rho\eta + 12\rho\eta^2 - 11\rho^2\eta + 5\rho^2\eta^2 + 5\rho^3\eta - \eta - 9\eta^2) \\
& + x^3t(1 - 6\rho + 5\rho^2 + 8\eta) + x^3t^2(8 - 5\eta) - 5x^3t^3 \\
& + x^3(-6\rho\eta + 5\rho^2\eta + \eta),
\end{aligned} \tag{259}$$

$$\begin{aligned}
\tilde{F}_\pm = & \sqrt{\eta} \mathcal{W}_\pm \left\{ \left[K_b (h_{1,\pm} + h_{2,\pm} \mathcal{W}_\pm^2) + G_b h_{3,\pm} \right] \delta(z_\pm) \right. \\
& \left. + K_b h_{4,\pm} \delta'(z_\pm) \right\},
\end{aligned} \tag{260}$$

where

$$\begin{aligned}
h_{1,\pm} = & -8xt\eta + 8x\eta^2 + 4x^2t + 12x^2\eta + 2x^3t - 2x^3\eta - 2x^4 - 16t\eta - 16\eta^2 \\
& - 4\sigma_\pm (6xt - 2x\eta + 3x^2t + x^2\eta - x^3 - 8t\eta - 4t^2 - 4\eta^2)
\end{aligned}$$

$$- 8\sigma_{\pm}^2 (3xt - x\eta - 5x^2 + 4t + 4\eta) + 16\sigma_{\pm}^3 (3x + t + \eta) , \quad (261)$$

$$\begin{aligned} h_{2,\pm} = & 2\sigma_{\pm} x (8t\eta^2 + 16t^2\eta + 8t^3 - 4xt\eta^2 + 4xt^3 - 8x^2t\eta - 6x^2t^2 - 2x^2\eta^2 \\ & - x^3t^2 + x^3\eta^2 + x^4t + x^4\eta) + 4\sigma_{\pm}^2 x (-4t\eta^2 - 8t^2\eta - 4t^3 \\ & - 12xt\eta - 8xt^2 - 4x\eta^2 + 2x^2t\eta - x^2t^2 + 3x^2\eta^2 + 3x^3t + 3x^3\eta) \\ & + 8\sigma_{\pm}^3 x (-4t\eta - 2t^2 - 2\eta^2 + 4xt\eta + xt^2 + 3x\eta^2 + 3x^2t + 3x^2\eta) \\ & + 16\sigma_{\pm}^4 x (2t\eta + t^2 + \eta^2 + xt + x\eta) , \end{aligned} \quad (262)$$

$$\begin{aligned} h_{3,\pm} = & -16xt\eta - 8xt + 8xt^2 + 8x\eta + 8x\eta^2 - 8x^2t + 8x^2\eta + 24t^2 - 24\eta^2 \\ & + 4\sigma_{\pm} (-10xt - 14x\eta - 5x^2t + 5x^2\eta - 4x^2 + 5x^3 + 12t - 4t^2 + 12\eta \\ & + 4\eta^2) + 16\sigma_{\pm}^2 (5x\eta - 2x + 5x^2 - 9t - 9\eta) \\ & + 80\sigma_{\pm}^3 (x + t + \eta) , \end{aligned} \quad (263)$$

$$\begin{aligned} h_{4,\pm} = & 4\sigma_{\pm} (4xt\eta - 4xt^2 + 6x^2t + 2x^2\eta + x^3t - x^3\eta - x^4 - 8t\eta - 8t^2) \\ & + 8\sigma_{\pm}^2 (8xt + 4x\eta + x^2t - 3x^2\eta - 3x^3 + 4t\eta + 4t^2) \\ & - 16\sigma_{\pm}^3 (xt + 3x\eta + 3x^2 - 2t - 2\eta) - 32\sigma_{\pm}^4 (x + t + \eta) , \end{aligned} \quad (264)$$

and

$$\mathcal{W}_{\pm} = \frac{1}{\sqrt{x(t + \eta)(2\sigma_{\pm} + x) - x^2t - (t + \eta)^2}} , \quad (265)$$

$$\mathcal{W} = \frac{1}{\sqrt{x(t + \eta)(x_{\nu 0} + x) - x^2t - (t + \eta)^2}} , \quad (266)$$

$$\sigma_{\pm} = (t - \eta)/(2\tau_{\pm}) , \quad z_{\pm} = 1 + t - \rho - x - 2\sigma_{\pm} . \quad (267)$$

The parameters K_b, G_b , representing the kinetic energy and the chromomagnetic energy, are defined according to [41]

7.5 Lepton energy distribution

As regards the HQET correction terms, we only give the energy distribution in the form of a diagram evaluated numerically. Beneath we also give the Born level approximation analytically. The analytic formulae for the polarized distribution can be simplified if we split the kinematical range of y into two parts, separated by the value of the charged lepton energy where the virtual W boson can stay at rest. This value is

$$x_W = 1 - \sqrt{\rho} + \frac{\eta}{1 - \sqrt{\rho}} . \quad (268)$$

In the formulae below, the superscripts A, B refer to the appropriate regimes:

$$x < x_W \quad \text{region } A , \quad (269)$$

$$x > x_W \quad \text{region } B . \quad (270)$$

The energy distribution of polarized τ lepton reads,

$$\frac{d\Gamma^{\pm}}{dx} = 12\Gamma_0 \left[\frac{1}{2} f(y) \pm \Delta f(x) \right] . \quad (271)$$

The function $f(x)$ represents the unpolarized case,

$$f(x) = \frac{1}{6} \zeta^2 \sqrt{x^2 - 4\eta} \left\{ \zeta [x^2 - 3y(1 + \eta) + 8\eta] + (3x - 6\eta)(2 - x) \right\} , \quad (272)$$

with

$$\zeta = 1 - \frac{\rho}{1 + \eta - x} . \quad (273)$$

The function $\Delta f(x)$ reads,

$$\Delta f(x) = \frac{3}{8} \sqrt{\eta|x-1|} \phi_1 \Psi + \frac{1}{4} \eta \phi_2 , \quad (274)$$

with

$$\begin{aligned} \phi_1 = & -5\lambda^3/(x-1)^4 + 3\lambda(4\eta - \lambda - \lambda^2)/(x-1)^3 + (4\eta\lambda - 4\eta + \lambda \\ & + 7\lambda^2 + \lambda^3)/(x-1)^2 + (-1 + 4\eta\lambda - 28\eta + 15\lambda - \lambda^2 - \lambda^3)/(x-1) \\ & - 1 + 12x\eta - 11x\lambda + 7x - x^2 + 12\eta\lambda - 24\eta + 14\lambda - 11\lambda^2 , \end{aligned} \quad (275)$$

$$\begin{aligned} \phi_2^A = & \sqrt{x^2 - 4\eta} \left[15\lambda^2\xi/(x-1)^3 + (10\eta\lambda\xi^2 - 16\eta\xi + 24\lambda\xi - 10\lambda\xi^2 \right. \\ & - 20\lambda - 6\lambda^2\xi)/(x-1)^2 + (-4 - 14\eta\lambda\xi^2 - 48\eta\xi + 66\eta\xi^2 - 24\eta\xi^3 \\ & + 8\eta^2\xi^3 - 76\lambda\xi + 14\lambda\xi^2 + 48\lambda + 3\lambda^2\xi + 25\xi - 26\xi^2 + 8\xi^3)/(x-1) \\ & \left. + 3 - 3x + 57\eta\xi - 22\eta\xi^2 - 12\lambda\xi - 21\lambda + 34\xi - 18\xi^2 + 8\xi^3 \right] , \end{aligned} \quad (276)$$

$$\begin{aligned} \phi_2^B = & 15\zeta\lambda^2/(x-1)^3 + (60\eta\zeta\lambda - 16\eta\zeta - 30\eta\zeta^2\lambda - 16\zeta\lambda - 21\zeta\lambda^2 \\ & + 10\zeta^2\lambda)/(x-1)^2 + (-104\eta\zeta\lambda - 84\eta\zeta + 52\eta\zeta^2\lambda + 122\eta\zeta^2 - 40\eta\zeta^3 \\ & + 160\eta^2\zeta - 160\eta^2\zeta^2 + 40\eta^2\zeta^3 - 24\zeta\lambda + 9\zeta\lambda^2 + 17\zeta - 4\zeta^2\lambda - 22\zeta^2 \\ & + 8\zeta^3)/(x-1) + 18 - 29x\eta + 27x\lambda - 21x + 3x^2 + 46\eta\zeta\lambda - 59\eta\zeta \\ & - 14\eta\zeta^2\lambda + 78\eta\zeta^2 - 16\eta\zeta^3 - 71\eta\lambda + 59\eta - 43\eta^2\zeta + 26\eta^2\zeta^2 - 8\eta^2\zeta^3 \\ & + 46\eta^2 - 6\zeta\lambda - 3\zeta\lambda^2 + 69\zeta - 6\zeta^2\lambda - 52\zeta^2 + 16\zeta^3 - 42\lambda + 24\lambda^2 \end{aligned} \quad (277)$$

where

$$\xi = 2 - \zeta , \quad \lambda = \rho + \eta . \quad (278)$$

The function Ψ can be written in the form,

$$\Psi = \begin{cases} \arccos \omega_{min} - \arccos \omega_{max} , & x < 1 \\ \operatorname{arccosh} \omega_{max} - \operatorname{arccosh} \omega_{min} , & x > 1 \end{cases} \quad (279)$$

with

$$\omega_{min,max} = \frac{2(x-1)t_{min,max} + x(x_m - x) - 2\eta}{x\sqrt{(x_m - x)^2 + 4\eta\rho}} . \quad (280)$$

Due to terms containing inverse powers of $(x-1)$ the expression (274) for $\Delta f(x)$ is apparently divergent at $x = 1$. However, expanding $\Delta f(x)$ in powers of $(x-1)$ for $x < 1$ and $x > 1$ one can check that this function is regular at $x = 1$.

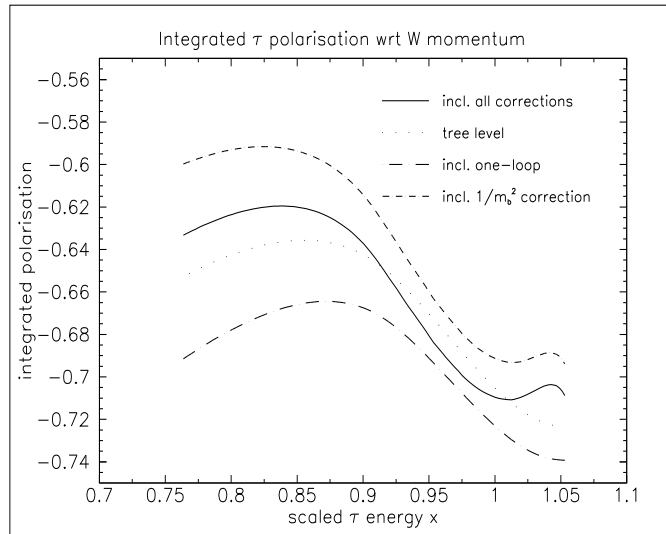


Figure 21: Integrated polarization of τ lepton along the direction of virtual W in the Born approximation (dot-dashed), including HQET corrections (long-dashed), perturbative corrections (short-dashed) and with both corrections included (solid) as functions of the scaled τ energy x . The mass of the b quark taken to be 4.75 GeV, c quark 1.35 GeV. The strong coupling constant $\alpha_s = 0.2$.

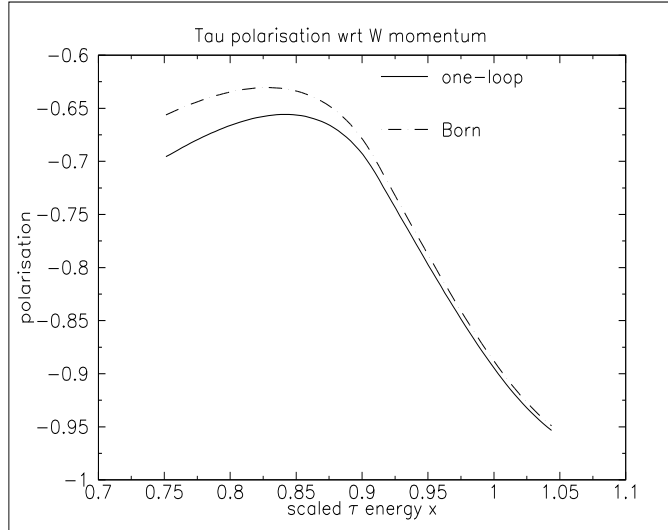


Figure 22: Polarisation of τ lepton along the direction of virtual W in the Born approximation (dashed) and including one loop corrections (solid) as functions of the scaled τ energy x . The mass of the b quark taken to be 4.75 GeV, c quark 1.35 GeV. $\alpha_s = 0.2$.

The HQET contribution to the decay distributions is known to render them unreliable near the endpoint values of the tauon energy. This ambiguity reveals itself in the polarisation as well. Similar problems appear also in calculations of perturbative corrections[32, 53]. All these problems are cured if instead of distributions their moments are considered[60, 59, 35]. In the case of τ polarisation a better defined quantity is the integrated polarisation

$$P_{int}(\bar{x}) = \int_{x_{min}}^{\bar{x}} dx \left(\frac{d\Gamma^+}{dx} - \frac{d\Gamma^-}{dx} \right) \Big/ \int_{x_{min}}^{\bar{x}} dx \left(\frac{d\Gamma^+}{dx} + \frac{d\Gamma^-}{dx} \right) \quad (281)$$

where both the lowest-order perturbative and the HQET terms are included. In Fig.21 the integrated polarisation is shown as a function of the scaled energy x of the τ lepton. The lowest order prediction corresponds to the dot-dashed line and the solid line is obtained including HQET and one-loop perturbative corrections. The latter have been evaluated numerically. The diagram also shows the effect of the perturbative corrections only. The perturbative correction to the polarisation is regular so there is no need to integrate over the scaled energy x . Fig. 22 shows the differential polarisation at tree level and including the one-loop correction. It is remarkable that this correction, though smaller in weight than the correction to the decay rate, is not suppressed to the extent that it is for the longitudinal polarisation. On the other hand, we see the two polarisations coincide at the endpoint where the energy of the tauon is large so

that its direction is almost equal to that of the pair of leptons. This is of course expected.

On integration over the whole range of the charged lepton energy one arrives at the total polarisation at the tree level corrected for the $O(1/m_b^2)$ effects as predicted by HQET. For $m_b = 4.75$ GeV and $m_c = 1.35$ GeV, we obtain

$$P = -0.7235 + 4.21 \frac{K_b}{m_b^2} + 1.48 \frac{G_b}{m_b^2} . \quad (282)$$

Taking $K_b = 0.15$ GeV², $G_b = -0.18$ GeV² and $\alpha_s = 0.2$ we obtain $P = -0.709$.

Although we are mostly concerned with the tau lepton polarisation here, the formulae derived in the present work may well be used in evaluating the polarisation of the light leptons. Interestingly, in the limit of a vanishing mass of the charged lepton the polarisation falls to zero apart from the endpoints, c.f. (274) and (253). It is due to the chiral $V - A$ structure of the weak charged current that, according to Eq.(145), the decay widths with a definite polarisation differ by a term proportional to $m_\tau s^\mu$. The polarisation four-vector of the charged lepton can be decomposed as follows:

$$s^\mu = (s^0, \vec{s}) = \left(\frac{p}{m} \sqrt{1 - (\vec{s}_\perp)^2}, \vec{s}_\perp, \frac{E}{m} \sqrt{1 - (\vec{s}_\perp)^2} \right) , \quad (283)$$

where \vec{s}_\perp is understood to mean the part of the three-vector \vec{s} perpendicular to the direction of the charged lepton. The quantities E and p denote, respectively, the energy and the three-momentum value of the charged lepton. This form can easily be seen to meet the definition of the polarisation four-vector. As the lepton mass approaches zero Eq.(283) gives

$$ms^\mu \approx \sqrt{1 - (\vec{s}_\perp)^2} \tau^\mu + m (0, \vec{s}_\perp, 0) . \quad (284)$$

However, if we want to keep the angle subtended by the polarisation vector and the lepton momentum constant the parallel part of the polarisation should be proportional to the perpendicular one, thereby forcing the factor of $\sqrt{1 - (\vec{s}_\perp)^2}$ to be of order of m/E . Then the r.h.s of Eq.(284) tends to zero for $m \rightarrow 0$. For the vanishing charged lepton mass the polarisation can be non-zero only where the virtual W boson is collinear with the charged lepton. In general the contribution to polarisation is appreciable only for W direction within the cone defined by the condition

$$|\vec{s}_\perp|/|\vec{s}| = \mathcal{O}(m/E) . \quad (285)$$

In particular this happens if p is much larger than the energy of the neutrino. For semitauonic B decays the condition (285) is satisfied in the whole phase space and the resulting polarisation is fairly large.

7.6 Summary

We have calculated the Born term and HQET first power correction to the polarisation of the τ meson with respect to the momentum of the intermediate

W boson. They are presented in an analytical form. Apart from that, the one-loop perturbative corrections have been evaluated numerically. In contrast to the longitudinal one, this polarisation receives noticeable corrections from perturbation expansion. All of the considered contributions have been presented in a diagram.

8 Summary

We have calculated a few quantities characterising the semileptonic decay of the B mesons. Perturbative and nonperturbative corrections have been found to the double distribution in terms of hadronic mass and electron energy for the decay $B \rightarrow X_u$ and to the polarisation of the τ lepton in the decay $B \rightarrow X_c$.

The longitudinal polarisation of the τ lepton receives only a tiny correction at one-loop level and it is nearly equal to the Born result to an excellent approximation. As such, this quantity may be of use in determining the quark mass differences.

The polarisation of τ is best measured with respect to the momentum of the intermediate W boson, so we have studied the appropriate distributions. We have found the leading HQET corrections of order $1/m_b^2$ analytically as well as computed numerically the one-loop perturbative corrections. The latter have turned out not to be negligible, contrary to the situation with the longitudinal polarisation.

The problem of measuring the V_{ub} matrix element has been addressed. We have proposed a quantity to be compared with experimental data and found the theoretical prediction for it including one-loop perturbative and leading twist nonperturbative corrections. The estimated error on the extracted value is 10%.

The results presented in this paper, save for the HQET corrections to the longitudinal polarisation, have been found for the first time in the papers [49]-[52].

9 Acknowledgements

I would like to thank my advisor, Professor Marek Jeżabek, for the guidance and many discussions. Thanks go also to Professor Maria Różańska for pointing out the need for calculating the τ polarisation, and Professor Thomas Mannel for elucidating aspects of HQET.

References

- [1] S. L. Glashow, Nucl. Phys. **22**, 579 (1961).
- [2] S. Weinberg, Phys. Rev. Lett. **19**, 1264 (1967).
- [3] A. Salam, in *Proceedings of the VIII Nobel Symposium*, edited by N. Svartholm, page 367, Almqvist and Wicksells, Stockholm, 1968.
- [4] R. P. Feynman, Phys. Rev. **76**, 769 (1949).
- [5] J. Schwinger, Phys. Rev. **74**, 1439 (1948).
- [6] J. Schwinger, Phys. Rev. **75**, 651 (1948).
- [7] R. E. Behrends, R. J. Finkelstein, and A. Sirlin, Phys. Rev. **101**, 866 (1956).
- [8] S. M. Berman, Phys. Rev. **112**, 267 (1958).
- [9] T. Kinoshita, Phys. Rev. Lett. **2**, 477 (1959).
- [10] T. Kinoshita, J. Math. Phys. **3**, 650 (1962).
- [11] T. D. Lee and M. Nauenberg, Phys. Rev. **133**, B1549 (1964).
- [12] M. A. Shifman and M. B. Voloshin, Sov. J. Nucl. Phys. **45**, 292 (1987).
- [13] M. A. Shifman and M. B. Voloshin, Sov. J. Nucl. Phys. **47**, 511 (1988).
- [14] H. D. Politzer and M. B. Wise, Phys. Lett. **B206**, 681 (1988).
- [15] H. D. Politzer and M. B. Wise, Phys. Lett. **B208**, 504 (1988).
- [16] N. Isgur and M. B. Wise, Phys. Lett. **B232**, 113 (1989).
- [17] N. Isgur and M. B. Wise, Phys. Lett. **B237**, 527 (1990).
- [18] E. Eichten and B. Hill, Phys. Lett. **B234**, 511 (1990).
- [19] E. Eichten and B. Hill, Phys. Lett. **B243**, 427 (1990).
- [20] B. Grinstein, Nucl. Phys. **B339**, 253 (1990).
- [21] H. Georgi, Phys. Lett. **B240**, 447 (1990).
- [22] M. Neubert, Phys. Rev. **D49**, 3392 (1994).
- [23] C. D. Froggatt and H. B. Nielsen, Nucl. Phys. **B147**, 277 (1979).
- [24] H. Fritzsch, Nucl. Phys. **B155**, 189 (1979).
- [25] S. Dimopoulos, L. J. Hall, and S. Raby, Phys. Rev. Lett. **68**, 1984 (1992).
- [26] H. Fritzsch and Z.-Z. Xing, Phys. Lett. **B413**, 396 (1997).
- [27] V. Fanti et al., Phys. Lett. **B465**, 335 (1999).
- [28] A. Alavi-Harati et al., Phys. Rev. Lett. **83**, 22 (1999).
- [29] S. J. Brodsky, G. P. Lepage, and P. B. Mackenzie, Phys. Rev. **D28**, 228 (1983).
- [30] G. Altarelli, N. Cabibbo, G. Corbo, L. Maiani, and G. Martinelli, Nucl. Phys. **B208**, 365 (1982).
- [31] J. Chay, H. Georgi, and B. Grinstein, Phys. Lett. **B247**, 399 (1990).

- [32] M. Jeżabek and J. H. Kühn, Nucl. Phys. **B320**, 20 (1989).
- [33] A. Ali and E. Pietarinen, Nucl. Phys. **B154**, 519 (1979).
- [34] A. Czarnecki, M. Jeżabek, and J. H. Kühn, Nucl. Phys. **B351**, 70 (1991).
- [35] A. Czarnecki, M. Jeżabek, and J. H. Kühn, Phys. Lett. **B346**, 335 (1995).
- [36] M. Jeżabek and L. Motyka, Acta Phys. Polon. **B27**, 3603 (1996).
- [37] M. Jeżabek and L. Motyka, Nucl. Phys. **B501**, 207 (1997).
- [38] M. Luke and A. V. Manohar, Phys. Lett. **B286**, 348 (1992).
- [39] I. I. Bigi, M. Shifman, N. G. Uraltsev, and A. Vainshtein, Phys. Rev. Lett. **71**, 496 (1993).
- [40] B. Blok, L. Koyrakh, M. Shifman, and A. I. Vainshtein, Phys. Rev. **D49**, 3356 (1994).
- [41] A. V. Manohar and M. B. Wise, Phys. Rev. **D49**, 1310 (1994).
- [42] S. Balk, J. G. Körner, D. Pirjol, and K. Schilcher, Z. Phys. **C64**, 37 (1994).
- [43] L. Koyrakh, Phys. Rev. **D49**, 3379 (1994).
- [44] L. A. Koyrakh, (1996).
- [45] A. F. Falk, Z. Ligeti, M. Neubert, and Y. Nir, Phys. Lett. **B326**, 145 (1994).
- [46] M. Różanska and K. Rybicki, Acta Phys. Polon. **B29**, 2065 (1998).
- [47] K. Kiers and A. Soni, Phys. Rev. **D56**, 5786 (1997).
- [48] M. Gremm, G. Köpp, and L. M. Sehgal, Phys. Rev. **D52**, 1588 (1995).
- [49] M. Jeżabek and P. Urban, Nucl. Phys. **B525**, 350 (1998).
- [50] P. Urban, Acta Phys. Polon. **B29**, 1429 (1998).
- [51] M. Jeżabek and P. Urban, Eur. Phys. J. **C11**, 317 (1999).
- [52] M. Jeżabek and P. Urban, Acta Phys. Polon. **B30**, 3353 (1999).
- [53] A. Czarnecki and M. Jeżabek, Nucl. Phys. **B427**, 3 (1994).
- [54] A. F. Falk, M. Luke, and M. J. Savage, Phys. Rev. **D53**, 6316 (1996).
- [55] M. Neubert, Nucl. Phys. Proc. Suppl. **59**, 101 (1997).
- [56] I. Bigi, M. Shifman, N. Uraltsev, and A. Vainshtein, Phys. Lett. **B328**, 431 (1994).
- [57] T. Mannel and S. Recksiegel, Phys. Rev. **D60**, 114040 (1999).
- [58] e. P. F. Harrison and e. H. R. Quinn, *The BaBar physics book: Physics at an asymmetric B factory*, Papers from Workshop on Physics at an Asymmetric B Factory (BaBar Collaboration Meeting), Rome, Italy, 11-14 Nov 1996, Princeton, NJ, 17-20 Mar 1997, Orsay, France, 16-19 Jun 1997 and Pasadena, CA, 22-24 Sep 1997.
- [59] M. B. Voloshin, Phys. Rev. **D51**, 4934 (1995).
- [60] A. Czarnecki, M. Jeżabek, J. G. Körner, and J. H. Kühn, Phys. Rev. Lett. **73**, 384 (1994).